



**HAL**  
open science

## High throughput genotyping of structural variations in a complex plant genome using an original Affymetrix® Axiom® array

Clement Mabire, Duarte Jorge, Aude Darracq, Ali Pirani, H el ene Rimbart, Delphine Madur, Valerie Combes, Cl ementine Vitte, S ebastien Praud, Nathalie Rivier e, et al.

### ► To cite this version:

Clement Mabire, Duarte Jorge, Aude Darracq, Ali Pirani, H el ene Rimbart, et al.. High throughput genotyping of structural variations in a complex plant genome using an original Affymetrix® Axiom® array. 2018. hal-02788790

**HAL Id: hal-02788790**

**<https://hal.inrae.fr/hal-02788790>**

Preprint submitted on 5 Jun 2020

**HAL** is a multi-disciplinary open access archive for the deposit and dissemination of scientific research documents, whether they are published or not. The documents may come from teaching and research institutions in France or abroad, or from public or private research centers.

L'archive ouverte pluridisciplinaire **HAL**, est destin ee au d ep ot et  a la diffusion de documents scientifiques de niveau recherche, publi es ou non,  emanant des  tablissements d'enseignement et de recherche fran ais ou  trangers, des laboratoires publics ou priv es.



Distributed under a Creative Commons Attribution - NonCommercial - NoDerivatives 4.0 International License

1 **High throughput genotyping of structural variations in a**  
2 **complex plant genome using an original Affymetrix®**  
3 **Axiom® array**  
4

5 Mabire Clément<sup>2\*</sup>, Duarte Jorge<sup>1\*</sup>, Aude Darracq<sup>2</sup>, Ali Pirani<sup>3</sup>, Hélène Rimbart<sup>1,4</sup>, Delphine Madur<sup>2</sup>,  
6 Valérie Combes<sup>2</sup>, Clémentine Vitte<sup>2</sup>, Sébastien Praud<sup>1</sup>, Nathalie Rivière<sup>1</sup>, Johann Joets<sup>2</sup>, Jean-Philippe  
7 Pichon<sup>1</sup>, Stéphane D. Nicolas<sup>2</sup>

8 \*Two authors contributed equally to work

9 Authors Affiliation:

10 1 Biogemma - Centre de Recherche de Chappes, CS 90126, Chappes 63720, France

11 2 GQE – Le Moulon, INRA, Univ. Paris-Sud, CNRS, AgroParisTech, Université Paris-Saclay, 91190 Gif-sur-  
12 Yvette, France

13 3 Thermo Fisher Scientific - 3450 Central Expy, Santa Clara, CA, 95051, USA

14 4 Present adress : GDEC, INRA, Université Clermont Auvergne, 63000 Clermont-Ferrand, France

15 Corresponding authors: [stephane.nicolas@inra.fr](mailto:stephane.nicolas@inra.fr)

16

17

18

# 19 Abstract

## 20 Background

21 Insertions/deletions (indels), and more specifically presence/absence variations (PAVs) are pervasive in  
22 maize and have strong functional and phenotypic effect by removing or modifying drastically genes.  
23 Genotyping of such variants on large panels remains poorly addressed, while necessary for approaches  
24 such as association mapping or genomic selection.

## 25 Results

26 We have developed a new high throughput and cost-effective tool to genotype indel. We first identified  
27 141,000 indels by aligning reads from the B73 line against the genome of three temperate maize inbred  
28 lines (F2, PH207, and C103) and reciprocally. Next, we designed an Affymetrix® Axiom® array to target  
29 these indels with a combination of probes selected at breakpoint sites (13%) and/or within the indel  
30 sequence either at polymorphic (25%) or non-polymorphic sites (63%) sites. The final array design is  
31 constituted of 662,772 probes and targets 105,927 indels including PAVs, ranging from 35bp to 129kbp.  
32 After Affymetrix® quality control, we successfully genotyped 89,393 indels (84%) on 445 maize DNA  
33 samples with 479,027 probes (72%). A principal coordinate analysis on dissimilarity estimated from a  
34 subset of 57,824 indels on 362 inbred lines is consistent with the structure obtained using 50K SNP  
35 arrays.

## 36 Conclusions

37 We efficiently genotyped thousands of small to large indels on a large number of individuals using a new  
38 Affymetrix® Axiom® array. This powerful tool opens the way to studying the contribution of indels to  
39 trait variation and heterosis in maize. The approach is easily extendable to other species and should  
40 contribute to decipher the biological impact of indels at a larger scale.

41

# 42 Keywords

43 Present Absent Variation, Copy Number Variation, Structural Variation, genotyping, array, Zea mays,  
44 Genome assembly, Breakpoint, Chromosomal rearrangements

45

46

47

# Introduction

48 In the past decade, there has been growing evidence that structural variations (SVs) are  
49 pervasive within plant genomes (Anderson et al., 2014; Beló et al., 2010; Cao et al., 2011; Liu et al.,  
50 2015; Owens et al., 2018; Saintenac et al., 2011; Saxena et al., 2014; Springer et al., 2009; Swanson-  
51 Wagner et al., 2010). Insertion/deletions (indels) are one class of SVs of particular interest since they  
52 lead to the presence or absence of, sometimes large, genomic regions at a given locus, among  
53 individuals from the same species. The content of these indels can either be present elsewhere in the  
54 genome, but can also be completely absent from the genome, in which case they are referred to as  
55 presence/absence variants (PAVs). Some indels carry entire genes or affect gene regulatory elements,  
56 and are thus likely to have a functional and phenotyping impact (Chia et al., 2012; Hirsch et al., 2014; Lu  
57 et al., 2015; Mace et al., 2013; Saxena et al., 2014). Hundreds to thousands of SVs, including PAVs and  
58 copy number variations (CNVs), have been discovered in several plant species, including wheat  
59 (Montenegro et al., 2017), rice (Zhao et al., 2018), *Arabidopsis thaliana* (Lu et al., 2012), Potato  
60 (Hardigan et al., 2016), pigeon peas (Varshney et al., 2017), and Sorghum (Shen et al., 2015). These  
61 results support the idea that one single reference genome cannot properly represent the complete gene  
62 set of a given species. There has been an increasing interest for building new individual genomes in  
63 complement to the reference genome, in order to better describe the genetic diversity within a plant  
64 species (Appels et al., 2018; Cao et al., 2011; Darracq et al., 2018; Hirsch et al., 2016; Jiao et al., 2017;  
65 Pinosio et al., 2016; Sun et al., 2018; Varshney et al., 2017; Zhou et al., 2017).

66 In maize, BAC sequence comparison first revealed that gene and transposable element content  
67 greatly vary between inbred lines (Fu and Dooner, (2002); Brunner et al. (2005)). Whole genome  
68 sequencing of the B73 inbred line then provided the opportunity to explore the extent of SVs across the  
69 entire maize genome (Schnable et al., 2009) by designing Comparative Genomic Hybridization (CGH)  
70 technology (Pinkel et al., 1998). Several CGH studies found multiple CNVs between the B73 reference  
71 genome and other maize inbred lines or teosintes (Beló et al., 2010; Springer et al., 2009; Swanson-  
72 Wagner et al., 2010). These studies demonstrated the large extent of SVs among maize inbred lines,  
73 including presence/absence variations of low copy sequences such as genes. This was well illustrated by  
74 the discovery of a large 2 Mbp presence/absence region between Mo17 and B73 carrying several genes  
75 (Beló et al., 2010; Hirsch et al., 2016; Springer et al., 2009; Swanson-Wagner et al., 2010). However, CGH  
76 array technology shows several major drawbacks since (i) it does not allow the discovery of sequences  
77 that are not present in the reference genome used for designing probes of the arrays, (ii) it has a limited  
78 resolution which does not allow detection of indels smaller than 1kb, and (iii) it is costly and labor-  
79 intensive, and therefore not adapted for genotyping several hundreds of individuals.

80 Methods based on SNP array experiments have been developed to detect CNVs and were shown  
81 to be more cost effective and with higher throughput but to reduce breakpoint resolution than CGH  
82 arrays (Cooper et al., 2008; Dellinger et al., 2010 Wang et al., 2017). Didion et al. (2012) identified  
83 atypical patterns of reduced hybridization intensities that were highly reproducible, so called “off-target  
84 variants” (OTVs). OTV patterns could originate either from the absence of the sequence due to a PAV  
85 polymorphism, or to a single nucleotide polymorphism within the probe sequence, thus preventing the

3

Comment citer ce document :

MABIRE, C., Jorge, Darracq, A., Pirani, A., Rimbart, Madur, D., Combes, V., Vitte, C., Praud, Rivière, Joets, J., Pichon, Nicolas Dimitri, S. (2018). High throughput genotyping of structural variations in a complex plant genome using an original Affymetrix® Axiom® array. BioRxiv. , DOI : 10.1101/507756

86 correct hybridization of the DNA sample. For instance, 45,974 OTVs were discovered in a maize  
87 population using the 600K Affymetrix® Axiom® SNP array (Unterseer et al., 2014). While these  
88 approaches proved to be useful, there is a strong risk of false positive detection of PAVs using OTV  
89 patterns, mainly because these arrays were not designed to target PAVs. In order to reduce this risk of  
90 false positive detection of PAVs and more largely CNVs, several methods based either on segmentation  
91 or Hidden Markov Chain have been developed to use variation of fluorescent intensity signal of  
92 contiguous probes along the genome (Hupe et al., 2004; Olshen et al., 2004; Picard et al., 2007, 2005,  
93 Marioni et al., 2006; Stjernqvist et al., 2007). These kind of approaches have been used on 600K  
94 Affymetrix® Axiom® SNP array to detect CNV and to explore the contribution of CNV to phenotypic  
95 variation (Lyra et al., 2018).

96 With the emergence of massive parallel sequencing, new methods have been developed to  
97 detect structural variations based on the alignment of resequencing reads onto a high quality reference  
98 genome sequence. Among these, three have been mainly used (Alkan et al., 2011): (i) the “read-depth”  
99 (RD) method which can only detect copy number variations, (ii) the “read-pair” (RP) method which can  
100 detect deletions as well as small insertions (up to the size of the insert), (iii) the “split-read” (SR) method  
101 which can also detect deletions and small insertions (up to the size of a read). Chia et al. (2012) used the  
102 RD approach to identify CNVs among 104 maize lines and performed association studies for several  
103 traits. However, the RD method does not allow the identification of novel sequences and is error prone,  
104 especially regarding the size of the discovered CNVs which greatly depends on the size of the sliding  
105 window used. The RP method has been implemented in many computational tools like BreakDancer  
106 (Chen et al., 2009) and has been widely used. Although it has proven to be highly efficient to detect  
107 deletions (Kidd et al., 2008; Korb et al., 2007; Tuzun et al., 2005), this approach suffers from two  
108 limitations: it does not allow precise detection of breakpoints and the size of the insertions which can be  
109 detected is directly limited by the library insert size. The SR method, which was first implemented in  
110 Pindel (Ye et al., 2009), has the advantage of defining breakpoints at a single base resolution, but again  
111 the size of the detectable inserted sequence is limited.

112 The “assembly” (AS) method is able to detect all types of SVs of any size, but is also the most  
113 cost and computation-intensive. It is the only method able to detect large insertions with precise  
114 breakpoint definition. However, the assembly of large and complex genomes such as maize remains very  
115 expensive and computationally intensive despite recent progress in this area (Darracq et al., 2018;  
116 Hirsch et al., 2016; Jiao et al., 2017). There has been in the past some attempts to reduce this complexity  
117 by reducing the number of sequences to assemble. For instance, Lai et al., (2010) identified 104  
118 deletions and 570 insertions among 6 maize inbred lines by assembling genomic regions from reads that  
119 did not map on the B73 reference genome. The sequences assembled by this approach were enriched in  
120 erroneous reads or reads coming from external contamination and they were too short to be anchored  
121 to the reference genome B73. Hirsch et al. (2014) identified several putatively expressed genes that  
122 were not present within B73 reference genome by assembling and comparing the transcriptome of  
123 hundreds of inbred lines. This new approach was limited to the transcribed part of the genome and  
124 suffered from a high level of false positives. More recently, Lu et al., 2015 used genotyping by  
125 sequencing approaches on 14,129 inbred lines to identify 1.1 million short and unique sequences (GBS

126 tags) that (i) did not align on the B73 reference genome or were aligned but outside of a 10Mbp  
127 windows around their mapped position, or (ii) were mapped at the same location by joint linkage  
128 mapping in NAM populations using co-segregation with SNP and logistic regression between indel and  
129 SNP in an association panel. The main drawback of this approach is the high percentage of missing data  
130 due to the low depth of sequencing which requires imputation before being able to make genetic  
131 analysis. Recent whole genome sequence assembly of PH207 (Hirsch et al., 2016), and F2 (Darracq et al.,  
132 2018) have allowed the identification of thousands of large indel and PAV sequences. For instance, 2,500  
133 genes were found either present or absent in PH207 and B73 genomes and 10,735 PAV sequences larger  
134 than 1kb were discovered between F2 and B73, including 417 novel genes in F2. These discovery  
135 approaches have been limited to a few individuals due to sequencing costs and computational  
136 challenges, so they have not been adapted for characterization of SVs on large maize panels. Darracq et  
137 al. (2018) developed an interesting approach for the genotyping of PAVs from mapping of low depth (5-  
138 20X) resequencing datasets. This method is based on the comparison of reads aligning to the region  
139 found in F2 and in the line of interest. While this method is potentially adapted to genotype PAVs on any  
140 set of line with low resequencing data, it has been so far used for PAV genotyping on a low (<30)  
141 number of maize lines. Moreover, it is restricted to the analysis of PAVs, and is not adapted for  
142 genotyping other types of SVs.

143 To our knowledge, no high-throughput genotyping approach has been developed for genotyping  
144 large numbers of indels, including PAVs, on a large sets of individuals. In this study, we present an  
145 approach which is both (i) comprehensive, as it includes the discovery and localization of deletions as  
146 well as insertions regarding the B73 reference genome at the base pair level and (ii) high throughput, as  
147 it allows to genotype thousands of indels on hundreds of individuals. Our strategy takes advantage of  
148 next generation sequencing (NGS) technologies and recent advances in assembly of complex genomes.  
149 It also benefits from the high efficiency of SNP arrays like the high-throughput Affymetrix® Axiom®  
150 technology. In this paper, we detail how we discovered thousands of small to large indels, including  
151 PAVs, from three maize inbred lines (F2, PH207 and C103) as compared to the B73 reference genome.  
152 We then describe how we designed and selected 600,000 probes to create a new Maize Affymetrix®  
153 Axiom® array to genotype these indels. Finally, we describe how we successfully used this array to  
154 genotype an association panel of 362 maize inbred lines.

155

# Results

156

## Indel and PAV discovery

157

158 To design a comprehensive indel genotyping array, we first needed to discover a set of indels  
159 which would be representative of the maize temperate germplasm. We already had access to sequence  
160 data for the European flint line F2 and we benefited from a first set of 42,330 F2-specific sequences  
161 larger than 150bp, and totaling 16Mb. This dataset was constituted from the *de novo* assembly of F2  
162 paired-end that failed (at least for one read of the pair) to align onto the B73 AGPv2 sequence and which  
163 were totally devoid of coverage by B73 reads (“Reference guided assembly” in Figure S2 so called “no  
164 map” approach). We also took advantage of the work done by Darracq et al., 2018 to add another  
165 10,044 F2-insertions (size >1 kb, total size of 88Mb) with less than 70% of their length covered by B73  
reads.

166

To complement these two datasets of F2/B73 deletions and insertions, we generated Illumina®  
167 paired-end and mate-pair sequences from two other key founders of temperate maize breeding  
168 programs: PH207 and C103. We then used these F2, PH207 and C103 sequence data to detect, not only  
169 PAVs this time, but all indels, at base pair resolution between these three lines and B73. This  
170 methodology allowed us to have access both to their sequences and their breakpoints allowing to  
171 genotype such indels in several individuals (See material and methods for more details).

172

We first aligned F2, PH207 and C103 sequences against the B73 reference genome sequence in  
173 order to detect deletions. Here, the term “deletion” does not reflect any underlying biological process of  
174 DNA excision, but refers to a sequence of at least 100bp present in the B73 genome at one locus and  
175 absent in another line at the same locus. Deletions were detected for the three lines simultaneously  
176 using the “genotyping” option of Pindel (Ye et al., 2009), generating a set of 26,368 non-redundant  
177 deletions with precise identification of their breakpoints (Figure S1 A). The number of deletions found  
178 for each line was similar, respectively 12,165, 11,922 and 13,432 for F2, PH207 and C103. 67% of the  
179 deletions found were unique to one line, 24% were shared by two lines and 9% by three lines. These  
180 results confirm the good complementarity of the lines chosen in this study.

181

Next, we generated a draft genome assembly for each of these lines, which were used as  
182 template for alignment of B73 reads to detect insertions regarding B73 reference genomes. As for  
183 deletions, here the term “insertion” does not reflect any underlying biological process of DNA  
184 integration, but defines a sequence larger than 100bp that is present in one line at a given locus, and  
185 absent from B73 at the same locus. These three draft assemblies cover less than one third of the  
186 expected maize genome size but include a large portion of low copy sequences, including genes, as  
187 shown by BUSCO results (Table 1). Detection of insertions was processed this time separately for each  
188 inbred line, and generated 28,221 insertions for F2, 27,904 insertions for C103 and 26,795 insertions for  
189 PH207, with their precise breakpoints. The number of insertions is similar between lines, but  
190 significantly greater than this obtained for deletions. Among these insertions, 26,691 cases could be  
191 uniquely anchored at base pair resolution onto the B73 reference genome sequence (Figure S1b). Again,

192 a majority of insertions were unique to one line (72%) confirming the complementarity of the material  
193 chosen.

194 Finally, the results from the different approaches were merged into a non-redundant set of  
195 141,325 indel sequences (see material and methods) comprising 52,175 deletions and 89,150 insertions.  
196 These regions were then used for the design of genotyping probes.

197

## 198 **Design of the genotyping array**

### 199 **Genotyping strategy**

200 Large indels can be efficiently genotyped with a SNP array using a combination of two types of  
201 probes: (i) “external” probes which target breakpoints using the two flanking sequences of a given indel  
202 (BP probes) and (ii) “internal” probes which target presence/absence regions (PARs) within the internal  
203 sequence of indels on polymorphic (OTV probes) or monomorphic sites (MONO probes). We define  
204 PARs as small portions of DNA sequence of at least 35bp that were observed present or absent at the  
205 genome level when comparing two individuals. They are thus suitable for the design of  
206 presence/absence genotyping probes. Ideally, each indel should be called by two BP probes on either  
207 side and by multiple internal probes regularly distributed along the internal sequence of the indel  
208 (Figure 1 A). However, in practice, this combination of different probes is not always possible. For  
209 instance, precise breakpoints were not described for all PAVs from our “No-map” approach and Darracq  
210 et al., 2018), and PARs for internal probes were not always found in our indels.

### 211 **Probe design**

212 On one hand, BP probes, which should behave like classical SNP probes where one allele  
213 corresponds to the presence and the other to the absence of the indel. They are useful to explore the  
214 conservation of the localization of large insertion/deletion events across multiple individuals, even when  
215 no internal probe can be designed due to the absence of PARs (Figure S6). Among the 141,325 selected  
216 variants, 86,406 indels (22,420 deletions and 63,986 insertions as compared to the B73 reference  
217 genome sequence) had breakpoints defined at base pair resolution and were suitable for BP probe  
218 design. Four different breakpoint types were identified according to the presence of micro-homology  
219 and/or shorter non homologous sequence (Muñoz-Amatriaín et al., 2013) in place of a complete deleted  
220 sequence (Figure S3): (type I) 3,397 cases with sharp breakpoints; (type II) 45,987 cases with a micro-  
221 homology sequence (8.6 bp on average and no more than 237 bp) which was present in one copy in the  
222 reference sequence and duplicated at both extremities of the novel inserted sequence; (type III) 36,893  
223 cases harboring insertion of a short non-homologous fragment (42.2 bp on average and up to 892 bp) in  
224 place of a large deleted sequence; and (type IV) 156 cases with a combination of type II and type III  
225 breakpoints. Following Affymetrix® recommendations, 19,010 indels with type II breakpoints having a  
226 micro-homology sequence longer than 5bp were excluded from the design process. In the end, 67,396  
227 indels, representing 48% of all available indel variants, were submitted to the Affymetrix® design  
228 pipeline. Two probes, one on forward (FW) and one on reverse (REV) strand, were designed for each



229 breakpoint. These probes were classified as *not possible* (18%), *not recommended* (33%), *neutral* (15%)  
230 and *recommended* (35%) by this automated pipeline (see Methods for details), leaving 33,430 indels  
231 (51%) that could be targeted by at least one *recommended* probe.

232 On the other hand, internal probes, which should behave like an “off-target” variants (Didion et  
233 al., 2012) where the hybridization of the probe stands for the presence and the absence of hybridization  
234 for the absence of the indel, are useful to explore the genetic diversity within indel sequences (Figure 1  
235 D). They will also be particularly interesting to target indels for which no breakpoint could be identified  
236 (such as PAVs from the “no map” approach).

237 For the design of OTV probes, we benefited from the availability of SNPs which had been  
238 previously identified from the alignment of resequencing data from a core collection of 25 temperate  
239 maize inbred lines against the B73-F2 maize pan-genome from Darracq et al. (2018). As a consequence,  
240 OTV probes have only been designed for deletions positioned on B73 reference genome and F2  
241 insertions coming from Darracq et al. (2018). Among these, the context sequences of 436,162 SNPs,  
242 corresponding to 21,390 indels, were extracted and submitted to Affymetrix® design pipeline. Again,  
243 two probes, one on forward (FW) and one on reverse (REV) strand, were designed for each SNP. Finally,  
244 a total of 872,324 OTV probes could be designed and scored as *not possible* (0.05%), *not recommended*  
245 (71%), *neutral* (14%) and *recommended* (16%), leaving 17,589 indels (82%) which could be targeted by at  
246 least one *recommended* probe.

247 For the design of BP and OTV probes we could rely on Affymetrix® design pipeline to identify  
248 probes localized in PARs and thus suitable for the Affymetrix® Axiom® technology. For the design of  
249 MONO probes, we first had to identify such PARs within 141,325 indels cumulating 133Mbp of  
250 sequence. We used sequence masking methods to exclude repeats based on similarity to known maize  
251 repeats or on occurrence of 17-mers found within the sequencing datasets we had for B73, F2, PH207  
252 and C103 (more details in methods). By doing so, we identified 122,972 PARs, representing a cumulated  
253 size of 27Mbp, corresponding to 20.3% of the initial size and allowing the possibility to design MONO  
254 probes for 79,987 indels (56.5%). These PAR sequences were successfully used for the design of  
255 25,735,797 MONO probes, among which 59% were scored as *recommended* and allowed to target  
256 62,875 indels (79%).

257 With this combined approach, we designed a total of 26,715,361 probes targeting 117,756  
258 indels, which represent a cumulated length of 250 Mbp including 27 Mbp of PARs (Table 2). Among  
259 these indels, 97,748 (83%) can only be targeted with either internal or external probes, but not both  
260 (Figure 3 A). These results support our overall strategy which includes the discovery of indels with  
261 precise breakpoints in a preliminary step, and the use of complementary internal/external probes for  
262 the genotyping of large indels.

## 263 **Array design**

264 We used the Affymetrix® recommendations to select the 700,000 probes to be included in the  
265 final array, plus some other criteria depending on the probe type. Nevertheless, because of their added  
266 value, we decided to keep all BP probes as soon as they had less than 3 hits on the B73 reference

267 genome sequence. This first selection consumed 84,994 probes targeting 53,456 indels, among which  
268 70% could only be targeted by BP probes. Concerning OTV and MONO probes, we first selected *neutral*  
269 and *recommended* probes having no hit at all (for insertions), and only one hit (for deletions), against  
270 the B73 reference genome sequence. We then considered their density with the objective to maximize  
271 the number of indels that could be surveyed, as well as to have an even distribution of probes along  
272 targeted indel sequences (see Methods for more details). We then performed a second selection among  
273 *not recommended* OTV and MONO probes for 4,541 indels that were still not targeted. After filtering  
274 some duplicated probes, we built a final array design containing 662,772 probes targeting 105,927  
275 indels that represent a cumulated length of 232 Mbp, including 25.9 Mbp of PARs.

## 276 **Description of the array content**

277 The final array design allows to genotype indels with various sizes, ranging from 37 bp to 129.7  
278 kbp, with a median of 501 bp (Figure S4). They are covered by 1 to 482 probes with a median of 3  
279 probes per indel (Figure S5). The number of probes does not always reflect the length of the indels, as  
280 the proportion of PARs within indels is highly variable. Indeed, while 8,040 indels (ranging from 37 bp to  
281 2,409 bp with a median of 163 bp) were completely covered by PARs and could thus be considered as a  
282 proper PAVs, 34,372 indels (ranging from 101 to 129,700 bp with a median of 320 bp) were not covered  
283 by any PAR at all (Figure 2). In fact, the number of internal probes were more strongly correlated to the  
284 size of the PARs ( $r^2 = 0.79$ ) rather than to the size of the indels ( $r^2 = 0.16$ ) (Figure S6).

285 As expected, the probe selection process did not impact the overall distribution of probe types  
286 among targeted indels as 35% of them can exclusively be genotyped by BP probes, whereas 50% can  
287 only be genotyped thanks to the use of internal probes, among which 73% are only targeted by the use  
288 of the original MONO probes (Figure 3b). Indeed, a large number of indels did not contain PARs and  
289 cannot be genotyped with 35bp internal probes but only with BP probes whereas some others indels  
290 contains PARs but have not BP due to Indel discovery approach (“No map”).

291 Among the 43,117 indels that could be anchored onto the B73 reference genome sequence and  
292 which were included in the array design, 13,737 were located inside a gene, 57 close to a gene (less than  
293 1 kb away), 1,311 inside a pseudogene and 2,212 inside a transposable element. From the localization of  
294 these indels, evaluated indels and probe density across each chromosome. We observed a higher  
295 density in chromosome arms than in peri-centromeric regions (Figure S7). We also identified clusters of  
296 indels with large specific sequence at the beginning of chromosome 6 (10-20Mbp) or at the end of  
297 chromosome 5 (~190Mbp).

## 298 **Assessing array quality by genotyping 105,927 indels on** 299 **480 maize DNA samples**

### 300 **Indel calling using dedicated Affymetrix® pipelines**

301 We genotyped 480 maize DNA samples including 440 inbred lines, 24 highly recombinant inbred  
302 lines and 16 F1 hybrids. Dedicated Affymetrix® pipelines were implemented for each of the probe types  
303 to call genotype of the indels based on fluorescent intensity and contrast variation of the probes. It

304 included two algorithms already developed by Affymetrix® (Didion et al., 2012) for BP and OTV probes  
305 (Figure S8 A et B) and a third one which was newly developed for the calling of presence/absence alleles  
306 using MONO probes (Figure 4). 35 DNA samples including all F1 hybrids, did not pass Affymetrix® quality  
307 control due to their low call rate (<0.9) and were eliminated. Out of 662,772 probes, 479,027 probes  
308 representing 89,393 indels (84%) passed Affymetrix® quality control and were called on 445 DNA  
309 samples. Respectively 55%, 59% and 81% of BP, OTV and MONO probes were converted into  
310 recommended markers after clustering by Affymetrix® pipelines (Table S1, S2, and S3). Thanks to the 3  
311 probe types and redundancy, 84% of indels could be called with an average of 5.4 probes per indel.

312 To evaluate the genotyping capacity of the probes, we first compared the clustering of inbred  
313 lines expected for three probe types (BP, OTV, and MONO) with the observed clustering of inbred lines  
314 based on fluorescence intensity and contrast of 445 inbred lines genotyped with the array. For BP  
315 probes, we expected at least two clusters corresponding to the individuals homozygous either for  
316 presence (“AA” or “BB”) or absence (“OO”). A third cluster could be observed when individuals were  
317 heterozygous individuals for presence/absence (“OA” or “OB” hemizygous) (Figure 1 C). For OTV probes,  
318 we expected at least 3 different clusters: two cluster corresponding to the individuals homozygous for  
319 allele A or B of SNP (“AA”, “BB”), and a third “off-target” cluster for the individuals homozygous for  
320 absence (“OO”). A fourth cluster could be observed when some individuals were heterozygous at the  
321 within-indel SNPs (AB). For MONO probes, we expected only two clusters corresponding to the  
322 individuals for which the sequence was present (“AA” or “BB”) or absent (“OO”, “AA” or “BB”) (Figure 1  
323 C). The observed clustering by the three dedicated pipelines was consistent with the expected clustering  
324 for 43% of BP, 83% of OTV and 63% of MONO probes (Table 3).

325 We observed also some unexpected clustering. For 57% of BP probes, we observed an additional  
326 off-target cluster (OTV in Table 3). This indicates that some BP probes did not hybridize properly in some  
327 inbred lines, which can either be due to the presence of polymorphism within flanking sequences of the  
328 targeted indels or to the existence of more complex rearrangements removing the breakpoints. To  
329 explore these two hypotheses, we took advantage of the availability of forward (FW) and reverse (REV)  
330 probes for 12,150 indels to determine whether the clustering between FW and REV BP probes from the  
331 same indel was similar or different. While 12% of these indels had their FW and REV BP probes classified  
332 identically either as OTV, 35% had their FW and REV probes classified differently (one as BP and the  
333 other as OTV).

334 Regarding MONO probes, 25% displayed additional cluster(s) when sequence were present  
335 suggesting the presence of a single nucleotide polymorphisms at this position. Among these, we were  
336 able to distinguish two types of clustering (Table 3). 4.7% of MONO probes exhibited a clustering similar  
337 to those observed for OTV probes suggesting that these MONO probes revealed really by chance a single  
338 nucleotide polymorphisms. In contrast, 20.4% of MONO probes displayed an unexpected clustering  
339 pattern for inbred lines with the presence of a heterozygous cluster but absence of a second  
340 homozygous cluster for SNP (Figure S12 B). In the end, 2.8% of MONO probes displayed an additional  
341 heterozygous cluster for SNP when sequence is present but no “off target” cluster corresponding to  
342 individuals for which sequence are absent (Figure S12 D)

343 For 18% of OTV (Figure S12 A) and 8.3% of MONO probes, clustering displayed no “off target”  
344 cluster for absence suggesting no presence/absence polymorphism at this position (Table 3). Note that  
345 some BP were also classified as monomorphic for presence/absence but were filtered out by the BP

346 pipeline (MonoHighResolution in Table S1).

347 Finally, 422,369 probes were able to call both presence and absence alleles, which allowed us to  
348 successfully genotype a total of 86,648 indels (82% of indels targeted by the array) on 445 inbred lines.

## 349 **Evaluation of genotyping reproducibility and quality**

### 350 *Consistency of genotyping among the four inbred lines used for indel discovery*

351 We used the 479,027 probes passing Affymetrix® quality controls to evaluate the quality of  
352 Presence/Absence genotyping by comparing the genotyping results from our array with those generated  
353 from sequencing data from the 4 lines used for the discovery of indels (B73, F2, PH207, and C103).  
354 Respectively 97.5%, 92.7% and 90.3% of the BP, OTV and MONO probes predicted a genotyping result  
355 consistent with this obtained with BLAST. We observed a strong asymmetry for concordance rate  
356 depending on whether we expect the locus to be present or absent from sequencing data (94.9% vs  
357 86.2% for allele present and absent, respectively). Interestingly, we observed no asymmetry for BP  
358 probes and a strong asymmetry for OTV and MONO probes for concordance rate (Table 4). The four  
359 inbred lines showed very similar concordance rates, F2 being the most concordant (97.9%). The median  
360 consistency rate of probes within indels remained relatively high and stable, around 90%, independently  
361 of the number of probes per indel (Figure S9).

### 362 *Consistency among probes from the same indel*

363 To estimate the consistency of different probes for typing a given indel, we analyzed genotyping  
364 results for 48,486 indels genotyped with at least two probes in a collection of 24 temperate inbred lines.  
365 Among these 24 lines, there are the four lines used to discover PAVs and the twenty used to discover  
366 SNPs within specific regions of Indels (Darracq et al., 2018). For each indel and each inbred line, we  
367 calculated the frequency of presence call over all probes. Frequencies of 1 (presence) and 0 (absence)  
368 indicated that all probes displayed consistent genotyping for the corresponding inbred line. Overall, 78%  
369 of these indels genotyping displayed an average allelic frequency for the presence allele of 1 or 0  
370 meaning that all probes had a consistent genotyping results for calling the allele at both present and  
371 absent states, respectively (Figure 5). A total of 12,308 indels (25%) displayed only two states across the  
372 24 inbred lines, corresponding to the presence or the absence of the sequence, while for 75% at least  
373 one inbred line had at least one inconsistent probe conducting to the presence of more than two  
374 haplotypes across 24 inbred lines. Some contradictory calls were repeatedly found across the 24  
375 samples (Figure S10), thus suggesting that some between-probe inconsistencies could have biological  
376 origins rather than being calling errors.

377 To investigate the consistency between the forward (FW) and reverse (REV) BP probes, we  
378 compared the genotyping results of 8,116 indels having both FW and REV BP probes called on our 24  
379 inbred lines. 33% of these indels have a consistent calling between their FW and REV probes for all  
380 inbred lines. The proportion of indels displaying an inconsistent calling between the FW and REV probes  
381 for 24 lines varied according to the breakpoint type and their classification (Figure S11). We observed  
382 also more similar calling when both FW and REV probes had similar classification (BP-BP or OTV-OTV)  
383 than when they had different classification status (BP-OTV) (Figure S11 A). Altogether, these results  
384 suggest that some calling inconsistencies could come from polymorphisms in the flanking sequence

385 while some other could be due to local rearrangements in the lines under genotyping as compared to  
386 the lines used for INDELs discovery.

### 387 *Assessing array quality to call highly hemizygous individuals using BP*

388 In order to evaluate our ability to identify individuals displaying hemizygous genotype  
389 (heterozygous for presence / absence of the sequence), we rescued for BP probes the genotyping of  
390 DNA samples for 12 F1 hybrid eliminated by Affymetrix® quality control due to their low call rate. This  
391 low call rate came mainly from inability of current Affymetrix® algorithms to identify hemizygous cluster  
392 for OTV and MONO probes and therefore to assign a genotype to hemizygous individuals. As a  
393 consequence, it strongly increase missing data for F1 hybrids only for OTV and MONO probes. We  
394 selected 20,370 BP probes classified as expected by the design (Table 3) to compare them with those  
395 expected from their 9 parental lines. 89% of observed homozygous alleles were consistent with  
396 expected genotyping results of F1 hybrids and 94% of observed hemizygous alleles were consistent with  
397 expected genotyping results.

### 398 *Reproducibility*

399 We evaluated the reproducibility of genotyping by comparing the genotyping results of 13  
400 different inbred lines that were replicated in the experiment (Table S4). Note that these are not perfect  
401 biological replicates as they represent the same variety but come either from different seed lots or from  
402 different accessions. These replicates exhibited a genotyping difference varying from 0.6% to 5.2%. This  
403 is similar to the amount of inconsistencies obtained on the same material using a 50K SNP array (Ganal  
404 et al., 2011) suggesting that indel genotyping inconsistencies for replicates come mostly from seed lot  
405 divergences rather than genotyping errors (Table S4).

406

## 407 **Application: Diversity analysis of 362 maize inbred lines** 408 **panel**

409 In order to evaluate the interest of this new array to analyze the contribution of indels to the  
410 genetic diversity, we analyzed 57,824 polymorphic indels among a subset of 362 out 445 inbred lines,  
411 representing a large genetic diversity and previously studied (Bouchet et al., 2013; Camus-Kulandaivelu,  
412 2005). To give same weight to each indel in the diversity analysis, we selected one single probe per indel  
413 based on the probe genotyping quality (see methods).

414 We first used these indels to calculate the genetic distance between inbred lines and to perform  
415 Principal Coordinate Analysis (PCoA) (Figure 6 A). To compare our indel-based results to this of  
416 previously characterized SNPs, we displayed on this PCoA the genetic structuration of these 362 inbred  
417 lines as obtained from the Panzea 50K SNP array (Bouchet et al., 2013). The first axis showed good  
418 discrimination of European Flint from Corn Belt Dent and Stiff Stalk lines, while the second axis  
419 discriminated European Flint and Northern Flint lines. Overall, the clustering of individuals based on  
420 genetic distance estimated with indels (1-IBS) by PCoA was consistent with the genetic structuration  
421 obtained from SNPs. We observed that B73 and F2, that were used to discover the majority of indels,

422 deviated from other inbred lines. We thus performed a second PCoA excluding B73 and F2 (Figure 6 B).  
423 The two PCoAs gave similar patterns.

424

# Discussion

425

## 1. An original high throughput approach for genotyping indels

426

427 The comparison of whole genome sequence assemblies is in theory the best approach to identify  
428 precisely and exhaustively structural variations between two individuals (Darracq et al., 2018; Hirsch et  
429 al., 2016; Jiao et al., 2017, Sun et al., 2018). But even though great progress has been made recently in  
430 this area, whole genome assembly is still too costly, time consuming and computationally intensive to be  
431 applied to hundreds of individual considering the complexity of maize genome (Darracq et al., 2018;  
432 Gabur et al., 2018). Other whole genome approaches based on sequencing and alignment of reads, and  
433 using “read-depth”, “read-pair” and “split-read” identification methods (Chen et al., 2009; Kidd et al.,  
434 2008; Korbel et al., 2007; Tuzun et al., 2005; Ye et al., 2009) were mostly limited to the identification of  
435 deletions (i.e. sequences absent compared to a reference genome). Liu et al., (2015) partially addressed  
436 the lack of insertions (i.e. novel sequences compared to a reference genome) in previous studies by the  
437 identification 1,973,746 indels. Although, among these a majority were very small (85% smaller than  
438 11bp) and the use of PCR markers to genotype them was time-demanding, labor-intensive and costly at  
439 large scale level. In this paper we describe an original approach combining the accuracy of the detection  
440 of insertions and deletions using high coverage sequence data and multiple reference genome  
441 assemblies, along with the high-throughput and accuracy of SNP arrays. We further show that using this  
442 approach, we were able to design and use an innovative array which allowed for the first time to  
443 genotype accurately thousands of small to large insertion/deletion variants, including PAVs, on  
444 hundreds of maize individuals. We used different methods to compile 52,175 deletions and 89,150  
445 insertions between three newly sequenced maize inbred lines (F2, PH207 and C103) and the maize B73  
446 AGPv2 reference genome, among which 75% were included in our array. Contrary to older studies, we  
447 did not focus solely on PAVs, but we also included in our array many insertion and deletion events, even  
448 if they contained non-unique sequences, by targeting their breakpoints.

449 By designing probes directly on indel breakpoints for both insertions and deletions , our approach  
450 overcomes some of the limitations of CGH or SNP array based studies. To our knowledge none of the  
451 previous studies which have used an array technology for genotyping indels have specifically targeted  
452 such a high number of insertion/deletion breakpoints. Unterseer et al., (2014) genotyped 6,759 small  
453 deletions which were discovered by aligning reads of 30 inbred lines against B73 genome but it included  
454 no insertions. However, CGH and SNP arrays did not usually design probes to target breakpoints and  
455 detected indels by analyzing the variation of fluorescent intensity signals of ordered probes (Cooper et  
456 al., 2008; Dellinger et al., 2010 Wang et al., 2017). As a consequence, these technologies targeted  
457 exclusively low copy regions of the genome excluding indels containing repeats such as TEs as soon as  
458 their breakpoints were not included in design (Beló et al., 2010; Lyra et al., 2018; Springer et al., 2009).  
459 This is a strong drawback for maize and many other crops since a large part of their sequence is  
460 composed of transposable elements (Feschotte et al., 2002; Schnable et al., 2009) that may be highly  
461 variable between individuals (Liu et al., 2015; Morgante et al., 2007; Sun et al., 2018) and may impact

462 phenotypes (Ducrocq et al., 2008; Salvi et al., 2007, 2002). Using BP probes allow to target  
463 Present/Absent Variation whose sequence were unique and not present elsewhere in the genome as  
464 well transposable elements whose their internal sequence could be present/absent at one locus but  
465 present elsewhere in the genome. Another advantage to genotype breakpoints is that we are almost  
466 certain to genotype the same mutational event across all individuals of the population because it is  
467 highly unlikely that two independent mutational events can lead to the same breakpoint. On the  
468 contrary, when we detected classically indels using CGH or SNP array, it is much harder to identify  
469 common indels among a population of individuals as we don't know precisely the breakpoint at base  
470 pair level. Genotyping breakpoint is also very cheap since only one or two probes by indel are required.  
471 Indel size is therefore no longer a limitation for genotyping using breakpoints in the contrary to SNP and  
472 CGH arrays which have limited resolution when they used fluorescent intensity variation (Alkan et al.,  
473 2011). The genotyping of breakpoints by sequencing is possible with a tool like Pindel (Ye et al., 2009)  
474 which has a genotyping mode, but at a much greater cost and with lower call rate compared to the use  
475 of an SNP array. Finally, breakpoint probes are codominant markers and allow to accurately genotype  
476 hemizygous individuals (Heterozygous for presence/absence) since their genotyping are based on  
477 fluorescent contrast rather than fluorescent intensity variation which are known to be more noisy as for  
478 MONO and OTV probes (Alkan et al., 2011).

479 Although the use of BP probes is clearly the simplest way to genotype indels using an SNP array,  
480 breakpoints are not always available (no maps approach discovery) or "designable" with 35bp probes,  
481 for instance when sequences of microhomology at breakpoint site were larger than 5bp. In order to  
482 genotype the 52,471 indels without breakpoints and explore the genetic diversity within indels, we also  
483 designed 577,778 internal probes both on monomorphic and polymorphic sites on PARs for both  
484 insertions and deletions. To genotype PARs in indel internal sequences using SNPs, we took advantage  
485 of the already available Affymetrix® algorithms to call Off-Target Variants (OTVs) which can detect  
486 variation of fluorescent intensity signals for a single probe (Didion et al., 2012) (Figure 1 C). This  
487 approach was used by Unterseer et al. (2014) who was able to detect 45,974 OTVs on a set of maize  
488 inbred lines using a 600K SNP array. Nevertheless, the array was designed in a classical way to target  
489 SNPs and there was no prior evidence that the probes called as OTVs would belong to real indels like in  
490 our approach. Additionally, detecting SNP in insertion required to assemble a pangenome combining  
491 common and specific sequence from different individuals in order to retrieve SNP by aligning reads from  
492 sequenced lines. In our case, the sole use of OTV probes would have conducted to the elimination of a  
493 lot of indels since 87,372 indels including 74,648 insertions had no known SNPs within their internal  
494 sequence. In order to avoid this ascertainment bias due to prior knowledge of the presence of SNPs, we  
495 designed 414,500 MONO probes on putative monomorphic sites within PARs of indel sequences. It  
496 permitted to genotype 38,134 supplementary indels that could be targeted neither by OTV or BP  
497 probes. This new type of probes required the development of a new algorithm in order to cluster  
498 individuals according to their fluorescent intensity variation only, to be able to assign a genotype to each  
499 individual (Figure 4). A limitation of current Affymetrix® algorithms to genotype indels using OTV and  
500 MONO probes is that they are currently unable to genotype hemizygous individuals. While it was not a  
501 strong issue for maize inbred lines (or individuals from autogamous species) that are mostly  
502 homozygous, it is a strong issue for individuals from allogamous species that are highly heterozygous. By



503 improving the current Affymetrix® algorithms, it should be possible to identify hemizygous cluster  
504 according to fluorescence intensity for OTV and MONO probes. We observed indeed some clusters that  
505 seem badly interpreted as heterozygote for SNP although they correspond more probably to  
506 hemizygous individuals for OTV and MONO probes (Figure S12B, see below for more detailed  
507 discussion). Alternatively, other algorithms/software based on fluorescent intensity variation of either a  
508 single probe or several ordered probes exists and could be used to detect copy number variation and  
509 therefore hemizygote in individuals (Hupe et al., 2004; Marioni et al., 2006; Olshen et al., 2004; Picard et  
510 al., 2007, 2005; Stjernqvist et al., 2007).

## 511 2. Reliability of genotyping / calling results

512  
513 Our approach provides a reliable and reproducible genotyping strategy for indels since (i) 91.5% of  
514 alleles called from probes are consistent with expected genotype from the resequencing data available  
515 for the 3 lines (F2, PH207, C103), (ii) 78% of indels genotyping had internal calls totally consistent  
516 between each other exhibiting either absence or presence for an inbred line, and (iii) the genotyping  
517 results were highly reproducible (94.8-99.4%) between biological replicates.

518 We observed a higher inconsistency between observed and expected calls for genotype “absent”  
519 than for genotype “present” with MONO and OTV probes, but not with BP probes (Table 4). This  
520 asymmetry between present and absent for consistency suggests a greater number of false positives in  
521 absent than present. We found that 20,574 indels were in fact totally monomorphic and present across  
522 all lines suggesting they represented false-positive indels coming certainly from regions which were not  
523 assembled in our draft genomes. Indeed, the probes targeting sequence regions present in one line but  
524 not assembled in their draft genome assembly, were falsely expected absent but they correctly  
525 hybridized with DNA and were called “present” on the array. This explains why the number of false  
526 positives was higher for B73, as all B73 absence genotypes were defined in comparison to draft  
527 assemblies, whereas for the other 3 lines absence genotypes were defined in comparison with the gold  
528 standard B73 genome sequence. The fact that we obtained a better result on OTV probes coming from  
529 F2 can be explained because we used only SNPs discovered on the B73-F2 pan-genome and not on other  
530 genomes. On the contrary, the fact that BP probes had similar consistencies for genotype “absent” and  
531 “present” could be explained because the BP probes were designed exclusively on B73 reference  
532 genome whatever we genotype insertions or deletions. One possible improvement to our approach to  
533 reduce the number of false-positive absences would be to not only align B73 reads onto each draft  
534 genome assembly but to align reads from each sequenced genomes on each other and against itself.  
535 This would have several benefits: (i) it would allow to discover even more indels and of better quality  
536 since each putative deletion discovered in one sample could potentially benefit from supporting reads  
537 from another sample, (ii) this would also simplify the identification of indels common to more than on  
538 genotype, and last but not least (iii) it would help to identify and eliminate false-positive deletions by  
539 the alignment of each sample on its own draft assembly.

540 Nevertheless, the use of incomplete draft genomes does not explain all discrepancies between  
541 expected and observed genotypes. First, these genotyping errors could also be due to a wrong clustering

542 leading to assign incorrectly genotype “present” instead of “absent” for a subset of individuals. It was  
543 well exemplified by some MONO probes classified as SNP although the clustering pattern looks like a  
544 MONO clustering with a strong difference of fluorescence intensity between two clusters. It suggests  
545 strongly for the cluster displaying the lowest fluorescent intensity a wrong assignment of homozygous  
546 genotype for one of two SNP alleles (presence of sequence) instead of the assignment of the  
547 homozygous absence of the sequence (Figure S12 C). Similarly, the more detailed inspection of the  
548 clustering of MONO probes displaying unexpected cluster pattern (Table 4, figure S12 D) and OTV  
549 probes classified as SNP (Table 4, figure S12 A) suggest a wrong assignment of genotype for the cluster  
550 displaying the lowest fluorescent intensity since the clustering looks like MONO and OTV clustering.  
551 Second, the genome divergence within probe sequence for some inbred lines could conduct to group  
552 those individuals in an OTV cluster and therefore lead this time to the assignment of an absent allele  
553 even though the sequence is present for these lines.

554 Surprisingly, 4.7% of MONO probes displayed a classical OTV clustering suggesting that an unknown  
555 SNP was targeted by these probes by chance. These 15,690 new OTVs are very interesting since they  
556 were discovered by chance on a large set of 445 inbred lines. We could therefore expect that these OTV  
557 have no ascertainment bias which can be very useful for analyzing genetic diversity within indels  
558 carrying PARs regions. On the contrary, 20.4% of MONO probes displayed an unexpected clustering with  
559 one off-target cluster corresponding to absence of the sequence, one cluster corresponding to  
560 heterozygous inbred lines for SNP but only one homozygous cluster (Unexpected MONO 1 in table 4).  
561 Considering these “unexpected MONO 1” as true SNP would conduct to a density of SNP (1 SNP every 5  
562 bp) which are not compatible with level of diversity observed in maize in different previous studies  
563 (Brandenburg et al., 2017; Gore et al., 2009). Deeper investigation of these MONO probes clustering  
564 showed for some probes that the cluster of heterozygous inbred lines displayed intermediate position  
565 for both intensity and contrast between two clusters homozygous for presence and absence of the  
566 sequence, respectively (Figure S12 B). It suggested strongly that these clusters of inbred lines assigned  
567 as heterozygous were in fact inbred lines carried only one copy of the sequence (hemizygous genotype).  
568 An alternative hypothesis to explain this unexpected pattern is the presence of divergent duplicated  
569 sequence leading to the presence of an artefactual heterozygous cluster for SNP corresponding to the  
570 presence of two paralogous sequences rather than one copy. This result suggests therefore that there is  
571 probably room to improve Affymetrix® algorithms in order to better identify additional clusters  
572 corresponding to the presence of hemizygous individuals for both MONO and OTV probes and therefore  
573 improve the quality of the genotyping of indels when using a SNP array.

574 These potential clustering errors as well as the bad design of some probes previously mentioned can  
575 explain that only 27% of indels displayed consistent genotype for presence/absence between all probes  
576 from same indels across the 24 inbred lines. Interestingly, some indels showed reproducible inconsistent  
577 genotypes for presence/absence across their probes in several inbred lines (Figure S10). It suggested  
578 that this pattern could not be due to random errors but could have instead a biological origin with  
579 possibly rearrangements having occurred several times within the same genomic region in some inbred  
580 lines. Following this hypothesis, Gu et al. (2008) observed two different types of rearrangement which  
581 could explain our observations: (i) rearrangements with an unique breakpoint in population and

582 therefore common size between individuals conducting to two haplotypes in a population (ii)  
583 rearrangement with non-unique breakpoints scattered in a genomic region which conducted to several  
584 haplotypes. This hypothesis is also supported in our experiment by the 56% of BP probes classified as  
585 OTVs indicating that FW or/and REV flanking sequence did not well hybridize in all lines.

586 The development of a statistical approach to merge either *a posteriori* the calling results of  
587 independent clustering of individual probes or *a priori* the fluorescent intensity signal of successive  
588 probes within a indel could be interesting in order to improve the robustness of indel genotyping. This  
589 would have the advantage to limit the effect of genotyping errors due to a bad clustering and to reduce  
590 the noise in fluorescent intensity signals. It would also help to identify true different haplotypes  
591 representative of the complexity of a region in a population.

592 Finally, 72% of probes were converted into markers, a number which is comparable to other maize  
593 Affymetrix® Axiom® SNP arrays in comparison to 74.9% in Unterseer et al., (2014). Out of these, only  
594 88% were really polymorphic for presence/absence. This conversion rate is not so bad considering that  
595 Affymetrix® Axiom® array analysis pipelines, which have been optimized for the detection of bi-allelic  
596 SNPs, are more sensitive to variations in fluorescent contrast (x-axis) compared to variations in  
597 fluorescent intensity (y-axis) which are known to be more noisy (Alkan et al., 2011; Didion et al., 2012).  
598 Moreover, we did not always followed Affymetrix® recommendations as we didn't filtered out probes  
599 with a bad design score.

600 To conclude, we developed a high-throughput and cost-effective indel genotyping array based on  
601 the indels discovered by sequencing on four inbred lines. It could be highly valuable to use more lines  
602 for the initial indel discovery step since our four inbred lines do not well represent the whole genomic  
603 diversity of maize, notably tropical lines. As a consequence, it could lead to ascertainment bias by  
604 reinforcing the differentiation of inbred lines genetically close to the four inbred lines used to discover  
605 indels (Clark et al., 2005; Ganal et al., 2011; Gouesnard et al., 2017) as we observed in our diversity  
606 analysis for lines close to B73 and F2. Several new individual maize genome assemblies are now  
607 available in the public domain and more and more could become available in the future. Our approach  
608 could easily be applied to these new genome assemblies to discover new indels on a larger set of inbred  
609 lines representative of maize diversity with the aim to design a new indel array. Although our arrays  
610 were not yet designed to genotype duplications and inversions, our approach could be easily extended  
611 to genotype breakpoints of inversions but required further development of pipeline for genotyping  
612 duplication using internal probes.

## 613 **Material and Methods**

### 614 **Indel and PAV discovery**

615 Three maize inbred lines, which are key founders of maize breeding program and originated  
616 from three different heterotic groups, have been selected for depth sequencing and indel discovery: the  
617 European Flint line F2 and two American dent lines, PH207 (Iodent) and C103 (Lancaster). DNA for

618 genotyping were extracted from leaves following a NaBisulfite method modified from Tai and Tanksley  
619 (1990) and Dellaporta et al. (1983). For each inbred line, paired-end and mate-pair whole genome  
620 shotgun libraries were sequenced on Illumina® HiSeq 2000 platforms (Table S6). A data set of B73  
621 paired-end reads (35x) was downloaded from the Sequence Read Archive (accession SRR404240).

622 For deletion discovery step, F2, PH207 and C103 paired-end reads were aligned against B73  
623 AGPv2 genome sequence using novoalign version 3.01.01 (<http://www.novocraft.com>) (default  
624 parameters). Samtools (Li et al., 2009) version 0.1.18 was used to coordinate sort and retain reads with  
625 a mapping quality of at least Q30. Duplicated reads were eliminated using MarkDuplicate from the  
626 picardtools suite (<http://broadinstitute.github.io/picard>) version 1.48. Pindel (Ye et al., 2009) version  
627 0.2.5a2 was ran in parallel on each chromosome to perform multi-genotype calling of deletions. Raw  
628 formatted results were converted to VCF (Variant Calling Format) standard format using the script  
629 Pindel2vcf. BreakDancer (Chen et al., 2009) was used in complement to Pindel but only for F2. Deletions  
630 shorter than 100bp were discarded. Deletions spanning a B73 assembly gap or located in regions prone  
631 to mis-assemblies such as telomeric, knob and centromeric regions, were also excluded from further  
632 analysis using IntersectBed BEDTools (Quinlan and Hall, 2010) version 2.16.1.

633 For whole genome sequence reconstruction of F2, PH207 and C103 inbred lines, paired-end and  
634 mate-pair reads were used together and assembled using ALLPATHs-LG (Gnerre et al., 2011) version  
635 R41008. For F2, the script CacheToAllPathsInputs.pl was used to cache the data to use for assembly:  
636 100% of the non-overlapping 230bp insert paired end data set, 100% of the overlapping 170bp insert  
637 paired end data set, 30% of the non-overlapping 370bp insert paired end data set, and 100% of the  
638 2.4kb insert mate pair data set. Indeed, only overlapping paired end reads are used by ALLPATHs-LG for  
639 building contigs, but the supplementary non-overlapping paired end reads for F2 was used for error  
640 correction. RunAllPathsLG was then run for all three genotypes using these optional parameters. For  
641 each assembly, the coverage of the gene space was evaluated using BUSCO (Waterhouse et al., 2018)  
642 version 3.0.2 using genome mode and maize species (-m geno -sp maize).

643 B73 paired-end reads were successively aligned to ALLPATHs-LG F2, PH207 and C103 genome  
644 sequence assemblies. The same tools and parameters used to call deletions against B73 genome were  
645 applied to detect B73 deletions against F2, PH207 and C103 genome sequences. For commodity, these  
646 B73 deletions will be reciprocally called insertions of F2, PH207 and C103 compared to B73 reference.  
647 Again, only insertions smaller than 100bp were discarded, but not the ones spanning assembly gaps as  
648 they were real assembly gaps (with approximate size inferred from paired reads average distance) and  
649 not “unsized” gaps like in B73 genome. When possible, insertions were anchored onto B73 AGPv2  
650 genome sequence using a dedicated pipeline combining Megablast version 2.2.19 (Altschul et al., 1990)  
651 and Age version 0.4 (<https://github.com/abzovlab/AGE>). Again, insertions that could be anchored on  
652 B73 reference and were overlapping regions prone to mis-assemblies such as telomeric, knob and  
653 centromeric regions, were also excluded from further analysis using IntersectBed.

654 F2 specific sequences coming either from the no-map approach (Figure S2) or from the work of  
655 Darracq et al. (2018) were included as such, without any further filtering.

656 The multiple references and approaches used during the indel discovery step led to a set of  
657 indels with various levels of redundancy. Some “intra-tool” redundancy was found (*eg.* multiple calls  
658 found by one tool within the same genotype at highly polymorphic loci). These “ambiguous” calls were  
659 systematically identified using the Bedtools suite version 2.16.1 (Quinlan and Hall, 2010) and eliminated.  
660 Moreover, for F2 deletions, some “inter-approach” redundancy was also expected and eliminated using  
661 intersectBed utility also from the Bedtools suite. When redundancy was found, Pindel calls were  
662 preferred to BreakDancer ones because they had precise breakpoints and contained also the calls for  
663 PH207 and C103. The same filter was applied to all insertions that could be anchored to the B73 genome  
664 sequence. Furthermore, for non-anchored indels, in order to avoid too much redundancy in internal  
665 genotyping probes design, RepeatMasker (<http://www.repeatmasker.org>) was used to mask redundant  
666 regions by similarity using an iterative approach. First, “ALLPATHs-LG assembly” F2 insertions were  
667 masked with “ABYSS assembly” F2 insertions (at least 95% of identity) to generate a non-redundant set  
668 of F2 insertions. Then C103 insertions were masked with F2 insertions (at 90% of identity), PH207  
669 insertions were masked with C103 and F2 insertions (90%), and finally F2 No-Map specific sequences  
670 were masked with PH207, C103 and F2 insertions (90%).

## 671 **Design of Affymetrix® Axiom® array**

### 672 **Preparation of sequences for probes for design**

673 To identify presence/absence regions (PARs) within indel sequences more suitable for the  
674 design of “off-target” probes, we used the genomtools Tallymer utility (Gremme et al., 2013) version  
675 1.5.6 to create two indexes for B73, F2, PH207 and C103: one from their genome assemblies (17-mers  
676 with a minimal occurrence of 1) and one from a 5x genome equivalent subset of their raw sequenced  
677 data (17-mers with a minimal occurrence of 5). Then B73 genome was iteratively annotated with the  
678 script tallymer2gff3.plx (options used: -k 17 -min 35 -occ 1|5 depending on the index) to identify regions  
679 not covered by F2, PH207 and C103 kmers. Reciprocally, the two F2 draft genomes, PH207 and C103  
680 ALLPATHs-LG draft genomes were ran through the same procedure to identify regions not covered by  
681 B73 kmers. The gff files generated by this process were then used in combination with gff files of  
682 repeats annotated with RepeatMasker to define PARs of a minimum size of 35bp for each type of indel  
683 and each draft genome.

### 684 **BP preparation**

685 Breakpoints could be targeted by probes (Figure 1 A) providing that the nucleotide flanking the  
686 breakpoint at the beginning of the deleted sequence were different from the nucleotide right after the  
687 end of deleted sequence (and reciprocally on the reverse strand). Type I and type III breakpoints without  
688 micro-homology sequence can be submitted to Affymetrix®’ straightforward design procedure whereas  
689 type II breakpoints have to go through an iterative design process, shifting the sequence by one base on  
690 each attempt until reaching a discriminative position. This iterative process stops after 5bp.

### 691 **Probes scoring**

692 All potential probes were evaluated in an in-silico analysis to predict their microarray  
693 performance. A p-conver value, which arises from a random forest model intended to predict the

694 probability that the SNP will convert on the array, was determined for all probes. The model considers  
695 factors including probe sequence, binding energies, and the expected degree of non-specific binding and  
696 hybridization to multiple genomic regions. This degree of non-specific binding is estimated calculating  
697 16-mer hit counts, which is the number of times all 16 bp sequences in the 30 bp flanking region from  
698 either side of the SNP have a matched sequence in the genome. These scores were generated both for  
699 forward and reverse probes. A probeset is recommended if  $p\text{-convert} \geq 0.6$  and there are no expected  
700 polymorphisms in the flanking region. A probeset is neutral if  $p\text{-convert} \geq 0.4$ , the number of expected  
701 polymorphisms in the flanking region is less than 3, and the polymorphisms are further than 21 bp of the  
702 variant of interest. Probesets not falling into these two categories are scored as *not recommended*.  
703 Probesets that cannot be designed are scored as *not possible*.

## 704 Probes selection

705 Concerning OTV and MONO probes, we applied three successive filtering steps. First, we  
706 selected only probes classified as recommended and neutral based their scoring, with no more than one  
707 hit on B73 reference genome for deletion probes and no hit at all for insertion probes were selected.  
708 After this step, 204,213 OTV probes and 18,884,827 MONO probes remained. Secondly, only probes  
709 with more than 70% in PARs were kept. An additional filtering step was implemented specifically for  
710 MONO probes to optimize probes distribution along the targeted PARs. To optimize probes distribution  
711 along the targeted PARs, these ones were cut in 75bp windows using windowmaker (Bedtools) and the  
712 MONO probe with the highest  $p\text{-convert}$  value was selected for each window. In case there were indels  
713 with less than 4 MONO probes selected using 75bp windows, these probes were eliminated and a  
714 second iteration was made using this time 50bp windows, followed by a last iteration with 25bp  
715 windows. This gave at this point a total of 616,286 probes including BP and OTV probes targeting  
716 108,703 indels (90% of indel selected for design).  
717 We completed the design by rescuing 6,219 OTV and 3,441 MONO probes from indels or PARs still not  
718 targeted by any probes, bringing the total number of probes selected to 625,946 to target 109,292 indel.  
719 At the last step, duplicated probeset were removed based on their sequence by Affymetrix® during the  
720 chip design procedure, leaving 662,772 probeset (105,927 indels) corresponding to 1,404,570 different  
721 probes to be arrayed on the array.

## 722 Genotyping of 105k indels on 480 maize DNA samples

### 723 Vegetal Material for genotyping

724 662,772 probes selected in the array were used to genotype 480 diverse DNA samples including  
725 440 inbred lines, 24 highly recombinant inbred lines and 16 F1 hybrids. Both F1 hybrids (obtained by  
726 crossing inbred lines) and their parental inbred lines were genotyped on the array but seed lots used to  
727 produce F1 hybrids and those used to extract DNA for genotyping were different. Among these 480  
728 DNAs, 13 inbred lines were genotyped using two different DNAs from two different seedlots and was  
729 used to evaluate the reproducibility of the genotyping (Table S4). DNA samples of one F1 hybrid were  
730 also genotyped 6 times.

731 DNA for genotyping were extracted from leaves following a NaBisulfite method modified from  
732 Tai and Tanksley (1990) and Dellaporta et al. (1983).

### 733 Variant calling using Affymetrix® algorithm

734 DNA samples from 480 individuals were hybridized to array using the Affymetrix® system. The  
735 genotyping, sample QC, and marker filtering was performed according to the Axiom® Best Practice  
736 genotyping analysis workflow. Genotype calls and classifications were generated from the hybridization  
737 signals in the form of CEL files using the Affymetrix® Power Tools (APT) and the SNPolisher package for R  
738 according to the Axiom® Genotyping Solution Data Analysis Guide.

739 The APT results were then post-processed using SNPolisher, which is an R package specifically  
740 designed by Affymetrix®. Markers metrics were generated using the *Ps\_Metrics* function. The markers  
741 QC metrics were used to classify probesets into 14 categories (Figure S13) using the *Ps\_Classification*  
742 and *Ps\_Classification\_Supplemental* functions with all default setting for diploid, except for an  
743 empirically determined, more stringent heterozygous variance filter (AB.varY.Z.cut=2.6). Example of  
744 clusters from each classification were visualized using the *Ps\_Visualization* function (Figure S13).

745 Each type of probe had a dedicated algorithm (Figure 4 and Figure S8) to call genotyping  
746 according to expected behavior from the probe design. Variant were preferentially selected as  
747 recommended if they were exhibiting stable category assignments with clearly separated clusters. Each  
748 variant was ranked into a category (Figure S13) at each step of the algorithm.

749 Algorithms used to convert BP and OTV were similar, as BP and OTV behaved like classical SNP.  
750 For initial genotype calling, a priori cluster position were used since no information about expected  
751 position was available. A first analysis was performed according to Affymetrix® recommendations.  
752 Secondly, level of inbreeding was taking into account for a posteriori cluster definition because of the  
753 high amount of inbred lines in the panel. This parameter took values from 0 for fully heterozygous to 16  
754 for completely homozygous samples. For OTV and BP algorithms, an inbred penalty of 4 (lower penalty  
755 for inbred species) was applied to try to re-labelled probes that fall into categories:  
756 CallRateBelowThreshold (CRBT), HomHomResolution (HHR), NoMinorHom (NMH), Other and  
757 UnexpectedHeterozygosity after the first cluster analysis. Markers that were classified as OTV may also  
758 be considered recommended after *OTV\_caller* function has been used to re-label the genotype calls. The  
759 SNPolisher *OTV\_Caller* function performed post-processing analysis to identify miscalled AB clustering  
760 and identify which samples should be in the OTV cluster and which samples should remain in the AA, AB,  
761 or BB clusters. Samples in the OTV cluster were re-labelled as OTV. Finally, the recommended markers  
762 list is created by combining the list of markers that are classified into the recommended categories  
763 (PolyHighResolution (PHR), MonoHighResolution (MHR), and OTV).

764 BP and OTV probes that exhibited only two clusters (AA or BB and OTV) should fall into  
765 monomorphic classification and classify as not recommended. A new MONO algorithm were developed  
766 (Figure 4) because we expected for this probes fluorescence pattern no polymorphism in the present  
767 sequence (Figure 1 C). Contrary to BP and OTV algorithm, *OTV\_caller* was used before inbred penalty for  
768 MONO probes analysis. To classify monomorphic sequence genotyping, the *OTV\_Caller* function was

769 called and as we expected monomorphic genotyping, only MHR and NMH were considered as  
770 recommended. Other monomorphic probes are then analyzed with an inbred penalty of 16 (highest  
771 level) to re-labelled probes considering maximum level of heterozygosity. Finally, a new function called  
772 *Hom2OTV* was used to classified probes exhibiting two homozygous clusters but with a different  
773 position in the Y axis (high and low position). This function tried to decide if the difference of contrast  
774 represent actually one homozygous and one OTV cluster as we expect (respectively presence and  
775 absence of the corresponding probe sequences). There are no parameters in this function. The lower  
776 intensity homozygous cluster is recalled as OTV.

## 777 Evaluation of genotyping quality

778 We compared the genotyping for 479,027 probes from indel array with expected genotyping from  
779 resequencing of 4 inbred lines used to discover indels: B73, F2, PH207 and C103. Expected genotyping  
780 was built from alignment of probes sequences on reference genome B73 and de novo assembly of 3  
781 inbred lines (F2, PH207 and C103) with Blast software. Sequences were considered present in lines when  
782 the probes were aligned with less than 5% of mismatch and absent when not.

783 Genotyping consistency for B73, F2, PH207 and C103 was calculated between expected and observed  
784 genotyping for “presence” and “absence” (Table 4). For this purpose, Affymetrix® genotyping was  
785 converted into two genotypes, present and absent and hemizygote from BP were considered as missing  
786 data. Consistency of Presence/Absence genotypes between resequencing and array genotyping was  
787 analyzed for four individuals (B73, F2, PH207, C103) according to probe types (BP, OTV, MONO):  
788 Number of similar genotypes between observed and expected/number of genotype observed. Note that  
789 the seed lot used for B73 and F2 genotyping is different from this used for indel discovery, while it is the  
790 same one for inbred lines PH207 and C103.

791 In order to evaluate the consistency of probes genotyping within indels (Figure 5), we used 24 inbred  
792 lines including 20 inbred lines from a core collection (Darracq et al., 2018) and the 4 inbred lines used for  
793 indel discovery. From 479,027 probes, we selected 294,650 polymorphic probes and totally consistent  
794 between sequencing and array genotyping in order to limit the genotyping errors due either to array or  
795 sequencing. These probes allowed us to genotyped 72,555 indels. We selected 48,486 polymorphic  
796 indels that are genotyped with at least two probes (corresponding to 270,581 probes), and calculated  
797 the frequency of presence allele for each indel and inbred lines.

798 To evaluate quality of genotyping for hybrids, we predicted the genotype of hybrids based on the  
799 genotyping of 2 parental lines for 20,370 BPs probes without OTV cluster. This expected genotype for  
800 hybrids was then compared with the observed genotyping from array of the corresponding hybrid. With  
801 following formula (Number of similar alleles (homozygous or hemizygous) between expected and  
802 observed)/(number of expected alleles (homozygous or hemizygous)).

803 To evaluate the reproducibility of the 479,027 probes of the array (Table S4), we compared genotyping  
804 of 13 duplicated inbred lines (A554, A632, A654, B73, C103, CO255, D105, EP1, F2, F252, KUI3, Oh43,  
805 and W117) originated from different seed sources. The genotyping of these 13 duplicated lines were  
806 also compared using 43,982 SNPs from the Illumina 50K SNP array.



## 807 **Diversity analysis**

808 We performed diversity analysis on 362 inbred lines from an association panel representing a  
809 wide range of diversity (Bouchet et al., 2013; Camus-Kulandaivelu, 2005) using genotyping from our  
810 indels Affymetrix® Axiom®. We compared these results with diversity analysis performed on same lines  
811 using genotyping of Illumina 50K SNP array (Ganal et al., 2011). Genotyping of indels were treated as bi-  
812 allelic 0/2 for “present” and “absent” respectively.

813 To perform diversity analysis, we first selected 237,629 probes among the 479,027 probes for  
814 which (i) the clustering observed were consistent with expected one (Table 3) and (ii) for which  
815 genotyping produced by our array for 4 lines used for discovered indels were totally consistent with  
816 genotyping based on the alignment of probes on genome assemblies using BLAST software. We filtered  
817 out 219,068 probes based on their genotyping quality (missing data rate below 20%, heterozygous rate  
818 below 15% and minor allele frequency above 5%). In the end, we selected a single probe by indels that  
819 are the best considering both genotyping and Affymetrix® quality leading to a set of 57,824 probes  
820 genotyping 57,824 indel to analyze diversity in 362 inbred lines.

821 We estimated two kinship matrices between 362 lines using “identity by state” estimators (IBS) based  
822 on 57,824 indels (Figure 6). Kinship matrices were estimated with the “ibd” function in R package  
823 GenABEL (Aulchenko et al., 2007). Genetic structuration were estimated using only 28,143 panzea SNPs  
824 using admixture software (Alexander et al., 2009). We selected Admixture results corresponding to five  
825 genetic groups (Q=5) since it corresponded to the number of genetics group defined in previous studies  
826 using panzea SNP from Illumina 50K (Bouchet et al., 2013). Lines were assigned to one genetic group  
827 providing that the probability of assignment to the groups were superior to 0.6 whereas lines below this  
828 threshold were considered “admixed”. In order to compare genetic structuration based on indels and  
829 SNP, we performed Principal Coordinate Analysis (PcoA) on genetic distance between lines with (362  
830 lines) and without F2 and B73 (360 lines) based on their dissimilarity (1-IBS) using Indels. Each lines were  
831 plotted on two first plan of PcoA and colored according to assignment to 5 genetics groups (Figure 6).

## 832 **Data Access**

833 The array content is available at <https://doi.org/10.15454/DWB4UT>

## 834 **Acknowledgements**

835 This work was supported by the project CNV-MAIZE (ANR-10-GENM-003) and the project Investement  
836 for the future AMAIZING ANR-10-BTBR-01 (ANR-PIA AMAIZING) and France Agrimer. PhD student C.  
837 Mabire is jointly funded by the program CNV4sel in the framework of metaprogram Selgen and by the  
838 Plant Biology and Breeding department of the French National Institute for Agricultural Research (INRA).  
839 We are very grateful to Patrick Schnable and Cheng-Ting “Eddy” Yeh to provide a subset of  
840 Presence/Absent Variants coming from their RNAseq and Sequence capture approach and for his helpful  
841 discussion. We are also very grateful to Alain Charcosset for his helpful discussion and comments on the  
842 manuscript.

## 843 **Disclosure declaration**

844 Ali Pirani is an employee of Affymetrix®.

## 845 **Authors' contributions**

846 SDN designed and supervised the study and conducted CNVMaize project

847 CM, JD and SDN drafted the manuscript, CV and JJ corrected the manuscript;

848 NR, SDN, JPP and SP conceived the array, AP, SDN, JJ and JD designed the array;

849 AP develop calling Affymetrix® pipelines and did the call of indel;

850 JPP, JJ and CV contributed to the sequencing;

851 JD, AD, HR and JJ performed the indel discovery, JD and JJ build genome assemblies, JJ and AD  
852 discovered SNP within indels;

853 CM evaluated the quality of genotyping and conducted genetic diversity analysis;

854 DM and VC did DNA extraction and prepared the samples for arrays genotyping;

855

856

# References

- 858 Alexander, D.H., Novembre, J., Lange, K., 2009. Fast model-based estimation of ancestry in unrelated  
859 individuals. *Genome Res.* 19, 1655–1664. <https://doi.org/10.1101/gr.094052.109>
- 860 Alkan, C., Coe, B.P., Eichler, E.E., 2011. Genome structural variation discovery and genotyping. *Nat. Rev.*  
861 *Genet.* 12, 363–376. <https://doi.org/10.1038/nrg2958>
- 862 Altschul, S.F., Gish, W., Miller, W., Myers, E.W., Lipman, D.J., 1990 Basic Local Alignment Search Tool 8.
- 863 Anderson, J.E., Kantar, M.B., Kono, T.Y., Fu, F., Stec, A.O., Song, Q., Cregan, P.B., Specht, J.E., Diers, B.W.,  
864 Cannon, S.B., et al., 2014. A Roadmap for Functional Structural Variants in the Soybean Genome.  
865 *G3* 4, 1307–1318. <https://doi.org/10.1534/g3.114.011551>
- 866 Appels, R., Eversole, K., Feuillet, C., Keller, B., Rogers, J., Stein, N., Pozniak, C.J., Stein, N., Choulet, F.,  
867 Distelfeld, A., et al., 2018. Shifting the limits in wheat research and breeding using a fully  
868 annotated reference genome. *Science* 361, eaar7191. <https://doi.org/10.1126/science.aar7191>
- 869 Aulchenko, Y.S., Ripke, S., Isaacs, A., van Duijn, C.M., 2007. GenABEL: an R library for genome-wide  
870 association analysis. *Bioinformatics* 23, 1294–1296.  
871 <https://doi.org/10.1093/bioinformatics/btm108>
- 872 Beló, A., Beatty, M.K., Hondred, D., Fengler, K.A., Li, B., Rafalski, A., 2010. Allelic genome structural  
873 variations in maize detected by array comparative genome hybridization. *Theor. Appl. Genet.*  
874 120, 355–367. <https://doi.org/10.1007/s00122-009-1128-9>
- 875 Bouchet, S., Servin, B., Bertin, P., Madur, D., Combes, V., Dumas, F., Brunel, D., Laborde, J., Charcosset,  
876 A., Nicolas, S., 2013. Adaptation of maize to temperate climates: mid-density genome-wide  
877 association genetics and diversity patterns reveal key genomic regions, with a major  
878 contribution of the Vgt2 (ZCN8) locus. *PLoS One* 8, e71377.
- 879 Brandenburg, J.-T., Mary-Huard, T., Rigail, G., Hearne, S.J., Corti, H., Joets, J., Vitte, C., Charcosset, A.,  
880 Nicolas, S.D., Tenaillon, M.I., 2017. Independent introductions and admixtures have contributed  
881 to adaptation of European maize and its American counterparts. *PLOS Genet.* 13, e1006666.  
882 <https://doi.org/10.1371/journal.pgen.1006666>
- 883 Brunner, S., 2005. Evolution of DNA Sequence Nonhomologies among Maize Inbreds. *PLANT CELL*  
884 *ONLINE* 17, 343–360. <https://doi.org/10.1105/tpc.104.025627>
- 885 Camus-Kulandaivelu, L., Veyrieras, J.B., Madur, D., Combes, V., Fourmann, M., Barraud, S., Dubreuil, P.,  
886 Gouesnard, B., Manicacci D., Charcosset A., 2005. Maize Adaptation to Temperate Climate: Relationship  
887 Between Population Structure and Polymorphism in the Dwarf8 Gene. *Genetics* 172, 2449–2463.  
888 <https://doi.org/10.1534/genetics.105.048603>
- 889 Cao, J., Schneeberger, K., Ossowski, S., Günther, T., Bender, S., Fitz, J., Koenig, D., Lanz, C., Stegle, O.,  
890 Lippert, C., et al., 2011. Whole-genome sequencing of multiple Arabidopsis thaliana populations.  
891 *Nat. Genet.* 43, 956–963. <https://doi.org/10.1038/ng.911>
- 892 Chen, K., Wallis, J.W., McLellan, M.D., Larson, D.E., Kalicki, J.M., Pohl, C.S., McGrath, S.D., Wendl, M.C.,  
893 Zhang, Q., Locke, D.P., et al., 2009. BreakDancer: an algorithm for high-resolution mapping of  
894 genomic structural variation. *Nat. Methods* 6, 677–681. <https://doi.org/10.1038/nmeth.1363>
- 895 Chia, J.-M., Song, C., Bradbury, P.J., Costich, D., de Leon, N., Doebley, J., Elshire, R.J., Gaut, B., Geller, L.,  
896 Glaubitz, J.C., Gore, M., et al., 2012. Maize HapMap2 identifies extant variation from a genome  
897 in flux. *Nat. Genet.* 44, 803–807. <https://doi.org/10.1038/ng.2313>
- 898 Clark, A.G., 2005. Ascertainment bias in studies of human genome-wide polymorphism. *Genome Res.*  
899 15, 1496–1502. <https://doi.org/10.1101/gr.4107905>
- 900 Cooper, G.M., Zerr, T., Kidd, J.M., Eichler, E.E., Nickerson, D.A., 2008. Systematic assessment of copy  
901 number variant detection via genome-wide SNP genotyping. *Nat. Genet.* 40, 1199–1203.  
902 <https://doi.org/10.1038/ng.236>

- 903 Darracq, A., Vitte, C., Nicolas, S., Duarte, J., Pichon, J.-P., Mary-Huard, T., Chevalier, C., Bérard, A., Le  
 904 Paslier, M.-C., Rogowsky, P., et al., 2018. Sequence analysis of European maize inbred line F2  
 905 provides new insights into molecular and chromosomal characteristics of presence/absence  
 906 variants. *BMC Genomics* 19. <https://doi.org/10.1186/s12864-018-4490-7>
- 907 Dellaporta, S.L., Wood, J., Hicks, J.B., 1983. A plant DNA minipreparation: Version II. *Plant Mol. Biol.*  
 908 *Report.* 1, 19–21. <https://doi.org/10.1007/BF02712670>
- 909 Dellinger, A.E., Saw, S.-M., Goh, L.K., Seielstad, M., Young, T.L., Li, Y.-J., 2010. Comparative analyses of  
 910 seven algorithms for copy number variant identification from single nucleotide polymorphism  
 911 arrays. *Nucleic Acids Res.* 38, e105–e105. <https://doi.org/10.1093/nar/gkq040>
- 912 Didion, J.P., Yang, H., Sheppard, K., Fu, C.-P., McMillan, L., de Villena, F.P.-M., Churchill, G.A., 2012.  
 913 Discovery of novel variants in genotyping arrays improves genotype retention and reduces  
 914 ascertainment bias. *BMC Genomics* 13, 34. <https://doi.org/10.1186/1471-2164-13-34>
- 915 Ducrocq, S., Madur, D., Veyrieras, J.-B., Camus-Kulandaivelu, L., Kloiber-Maitz, M., Presterl, T.,  
 916 Ouzunova, M., Manicacci, D., Charcosset, A., 2008. Key Impact of Vgt1 on Flowering Time  
 917 Adaptation in Maize: Evidence From Association Mapping and Ecogeographical Information.  
 918 *Genetics* 178, 2433–2437. <https://doi.org/10.1534/genetics.107.084830>
- 919 Feschotte, C., Jiang, N., Wessler, S.R., 2002. Plant transposable elements: where genetics meets  
 920 genomics. *Nat. Rev. Genet.* 3, 329–341. <https://doi.org/10.1038/nrg793>
- 921 Fu, H., Dooner, H.K., 2002. Intraspecific violation of genetic colinearity and its implications in maize.  
 922 *Proc. Natl. Acad. Sci.* 99, 9573–9578.
- 923 Gabur, I., Chawla, H.S., Snowdon, R.J., Parkin, I.A.P., 2018. Connecting genome structural variation with  
 924 complex traits in crop plants. *Theor. Appl. Genet.* <https://doi.org/10.1007/s00122-018-3233-0>
- 925 Ganal, M.W., Durstewitz, G., Polley, A., Bérard, A., Buckler, E.S., Charcosset, A., Clarke, J.D., Graner, E.-  
 926 M., Hansen, M., Joets, J., et al., 2011. A Large Maize (*Zea mays* L.) SNP Genotyping Array:  
 927 Development and Germplasm Genotyping, and Genetic Mapping to Compare with the B73  
 928 Reference Genome. *PLoS ONE* 6, e28334. <https://doi.org/10.1371/journal.pone.0028334>
- 929 Gnerre, S., MacCallum, I., Przybylski, D., Ribeiro, F.J., Burton, J.N., Walker, B.J., Sharpe, T., Hall, G., Shea,  
 930 T.P., Sykes, S., et al., 2011. High-quality draft assemblies of mammalian genomes from massively  
 931 parallel sequence data. *Proc. Natl. Acad. Sci.* 108, 1513–1518.  
 932 <https://doi.org/10.1073/pnas.1017351108>
- 933 Gore, M.A., Chia, J.-M., Elshire, R.J., Sun, Q., Ersoz, E.S., Hurwitz, B.L., Peiffer, J.A., McMullen, M.D.,  
 934 Grills, G.S., Ross-Ibarra, J., et al., 2009. A First-Generation Haplotype Map of Maize. *Science* 326,  
 935 1115–1117. <https://doi.org/10.1126/science.1177837>
- 936 Gouesnard, B., Negro, S., Laffray, A., Glaubitz, J., Melchinger, A., Revilla, P., Moreno-Gonzalez, J., Madur,  
 937 D., Combes, V., Tollon-Cordet, et al., 2017. Genotyping-by-sequencing highlights original  
 938 diversity patterns within a European collection of 1191 maize flint lines, as compared to the  
 939 maize USDA genebank. *Theor. Appl. Genet.* 130, 2165–2189. <https://doi.org/10.1007/s00122-017-2949-6>
- 940
- 941 Gremme, G., Steinbiss, S., Kurtz, S., 2013. GenomeTools: A Comprehensive Software Library for Efficient  
 942 Processing of Structured Genome Annotations. *IEEE/ACM Trans. Comput. Biol. Bioinform.* 10,  
 943 645–656. <https://doi.org/10.1109/TCBB.2013.68>
- 944 Gu, W., Zhang, F., Lupski, J.R., 2008. Mechanisms for human genomic rearrangements. *PathoGenetics* 1,  
 945 4. <https://doi.org/10.1186/1755-8417-1-4>
- 946 Hardigan, M.A., Crisovan, E., Hamilton, J.P., Kim, J., Laimbeer, P., Leisner, C.P., Manrique-Carpintero,  
 947 N.C., Newton, L., Pham, G.M., Vaillancourt, B., et al., 2016. Genome Reduction Uncovers a Large  
 948 Dispensable Genome and Adaptive Role for Copy Number Variation in Asexually Propagated  
 949 *Solanum tuberosum*. *Plant Cell* 28, 388–405. <https://doi.org/10.1105/tpc.15.00538>

- 950 Hirsch, C.N., Foerster, J.M., Johnson, J.M., Sekhon, R.S., Muttoni, G., Vaillancourt, B., Penagaricano, F.,  
 951 Lindquist, E., Pedraza, M.A., Barry, K., et al., 2014. Insights into the Maize Pan-Genome and Pan-  
 952 Transcriptome. *Plant Cell* 26, 121–135. <https://doi.org/10.1105/tpc.113.119982>
- 953 Hirsch, C.N., Hirsch, C.D., Brohammer, A.B., Bowman, M.J., Soifer, I., Barad, O., Shem-Tov, D., Baruch, K.,  
 954 Lu, F., Hernandez, A.G., et al., 2016. Draft Assembly of Elite Inbred Line PH207 Provides Insights  
 955 into Genomic and Transcriptome Diversity in Maize. *Plant Cell* 28, 2700–2714.  
 956 <https://doi.org/10.1105/tpc.16.00353>
- 957 Hupe, P., Stransky, N., Thiery, J.-P., Radvanyi, F., Barillot, E., 2004. Analysis of array CGH data: from  
 958 signal ratio to gain and loss of DNA regions. *Bioinformatics* 20, 3413–3422.  
 959 <https://doi.org/10.1093/bioinformatics/bth418>
- 960 Jiao, Y., Peluso, P., Shi, J., Liang, T., Stitzer, M.C., Wang, B., Campbell, M.S., Stein, J.C., Wei, X., Chin, C.-S.,  
 961 et al., 2017. Improved maize reference genome with single-molecule technologies. *Nature*.  
 962 <https://doi.org/10.1038/nature22971>
- 963 Kidd, J.M., Cooper, G.M., Donahue, W.F., Hayden, H.S., Sampas, N., Graves, T., Hansen, N., Teague, B.,  
 964 Alkan, C., Antonacci, F., et al., 2008. Mapping and sequencing of structural variation from eight  
 965 human genomes. *Nature* 453, 56–64. <https://doi.org/10.1038/nature06862>
- 966 Korbel, J.O., Urban, A.E., Affourtit, J.P., Godwin, B., Grubert, F., Simons, J.F., Kim, P.M., Palejev, D.,  
 967 Carriero, N.J., Du, L., et al., 2007. Paired-End Mapping Reveals Extensive Structural Variation in  
 968 the Human Genome. *Science* 318, 420. <https://doi.org/10.1126/science.1149504>
- 969 Lai, J., Li, R., Xu, X., Jin, W., Xu, M., Zhao, H., Xiang, Z., Song, W., Ying, K., Zhang, M., 2010. Genome-wide  
 970 patterns of genetic variation among elite maize inbred lines. *Nat. Genet.* 42, 1027.
- 971 Li, H., Handsaker, B., Wysoker, A., Fennell, T., Ruan, J., Homer, N., Marth, G., Abecasis, G., Durbin, R.,  
 972 1000 Genome Project Data Processing Subgroup, 2009. The Sequence Alignment/Map format  
 973 and SAMtools. *Bioinformatics* 25, 2078–2079. <https://doi.org/10.1093/bioinformatics/btp352>
- 974 Liu, J., Qu, J., Yang, C., Tang, D., Li, J., Lan, H., Rong, T., 2015. Development of genome-wide insertion  
 975 and deletion markers for maize, based on next-generation sequencing data. *BMC Genomics* 16.  
 976 <https://doi.org/10.1186/s12864-015-1797-5>
- 977 Lu, F., Roday, M.C., Glaubitz, J.C., Bradbury, P.J., Elshire, R.J., Wang, T., Li, Yu, Li, Yongxiang, Semagn, K.,  
 978 Zhang, X., et al., 2015. High-resolution genetic mapping of maize pan-genome sequence  
 979 anchors. *Nat. Commun.* 6. <https://doi.org/10.1038/ncomms7914>
- 980 Lu, P., Han, X., Qi, J., Yang, J., Wijeratne, A.J., Li, T., Ma, H., 2012. Analysis of Arabidopsis genome-wide  
 981 variations before and after meiosis and meiotic recombination by resequencing *Landsberg*  
 982 *erecta* and all four products of a single meiosis. *Genome Res.* 22, 508–518.  
 983 <https://doi.org/10.1101/gr.127522.111>
- 984 Lyra, D.H., Galli, G., Alves, F.C., Granato, Í.S.C., Vidotti, M.S., Bandeira e Sousa, M., Morosini, J.S., Crossa,  
 985 J., Fritsche-Neto, R., 2018. Modeling copy number variation in the genomic prediction of maize  
 986 hybrids. *Theor. Appl. Genet.* <https://doi.org/10.1007/s00122-018-3215-2>
- 987 Mace, E.S., Tai, S., Gilding, E.K., Li, Y., Prentis, P.J., Bian, L., Campbell, B.C., Hu, W., Innes, D.J., Han, X., et  
 988 al., 2013. Whole-genome sequencing reveals untapped genetic potential in Africa’s indigenous  
 989 cereal crop sorghum. *Nat. Commun.* 4. <https://doi.org/10.1038/ncomms3320>
- 990 Marioni, J.C., Thorne, N.P., Tavare, S., 2006. BioHMM: a heterogeneous hidden Markov model for  
 991 segmenting array CGH data. *Bioinformatics* 22, 1144–1146.  
 992 <https://doi.org/10.1093/bioinformatics/btl089>
- 993 Montenegro, J.D., Golicz, A.A., Bayer, P.E., Hurgobin, B., Lee, H., Chan, C.-K.K., Visendi, P., Lai, K., Doležel,  
 994 J., Batley, J., Edwards, D., 2017. The pangenome of hexaploid bread wheat. *Plant J.* 90, 1007–  
 995 1013. <https://doi.org/10.1111/tpj.13515>
- 996 Morgante, M., Depaoli, E., Radovic, S., 2007. Transposable elements and the plant pan-genomes. *Curr.*  
 997 *Opin. Plant Biol.* 10, 149–155. <https://doi.org/10.1016/j.pbi.2007.02.001>

- 998 Muñoz-Amatriaín, M., Eichten, S.R., Wicker, T., Richmond, T.A., Mascher, M., Steuernagel, B., Scholz, U.,  
 999 Ariyadasa, R., Spannagl, M., Nussbaumer, T., et al., 2013. Distribution, functional impact, and  
 1000 origin mechanisms of copy number variation in the barley genome. *Genome Biol.* 14.  
 1001 <https://doi.org/10.1186/gb-2013-14-6-r58>
- 1002 Olshen, A.B., Venkatraman, E.S., Lucito, R., Wigler, M., 2004. Circular binary segmentation for the  
 1003 analysis of array-based DNA copy number data. *Biostatistics* 5, 557–572.  
 1004 <https://doi.org/10.1093/biostatistics/kxh008>
- 1005 Owens, G.L., Baute, G.J., Hubner, S., Rieseberg, L.H., 2018. Genomic sequence and copy number  
 1006 evolution during hybrid crop development in sunflowers. *Evol. Appl.*  
 1007 <https://doi.org/10.1111/eva.12603>
- 1008 Picard, F., Robin, S., Lavielle, M., Vaisse, C., Daudin, J.-J., 2005. A statistical approach for array CGH data  
 1009 analysis. *BMC Bioinformatics* 14.
- 1010 Picard, F., Robin, S., Lebarbier, E., Daudin, J.-J., 2007. A Segmentation/Clustering Model for the Analysis  
 1011 of Array CGH Data. *Biometrics* 63, 758–766. <https://doi.org/10.1111/j.1541-0420.2006.00729.x>
- 1012 Pinkel, D., Seagraves, R., Sudar, D., Clark, S., Poole, I., Kowbel, D., Collins, C., Kuo, W.-L., Chen, C., Zhai, Y.,  
 1013 et al., Albertson, D.G., 1998. High resolution analysis of DNA copy number variation using  
 1014 comparative genomic hybridization to microarrays. *Nat. Genet.* 20, 207–211.  
 1015 <https://doi.org/10.1038/2524>
- 1016 Pinosio, S., Giacomello, S., Faivre-Rampant, P., Taylor, G., Jorge, V., Le Paslier, M.C., Zaina, G., Bastien, C.,  
 1017 Cattonaro, F., Marroni, F., Morgante, M., 2016. Characterization of the Poplar Pan-Genome by  
 1018 Genome-Wide Identification of Structural Variation. *Mol. Biol. Evol.* 33, 2706–2719.  
 1019 <https://doi.org/10.1093/molbev/msw161>
- 1020 Quinlan, A.R., Hall, I.M., 2010. BEDTools: a flexible suite of utilities for comparing genomic features.  
 1021 *Bioinformatics* 26, 841–842. <https://doi.org/10.1093/bioinformatics/btq033>
- 1022 Sainenac, C., Jiang, D., Akhunov, E.D., 2011. Targeted analysis of nucleotide and copy number variation  
 1023 by exon capture in allotetraploid wheat genome. *Genome Biol.* 12, R88.
- 1024 Salvi, S., Sponza, G., Morgante, M., Tomes, D., Niu, X., Fengler, K.A., Meeley, R., Ananiev, E.V., Svitashv,  
 1025 S., Bruggemann, E., et al., 2007. Conserved noncoding genomic sequences associated with a  
 1026 flowering-time quantitative trait locus in maize. *Proc. Natl. Acad. Sci.* 104, 11376–11381.  
 1027 <https://doi.org/10.1073/pnas.0704145104>
- 1028 Salvi, S., Tuberosa, R., Chiapparino, E., Maccaferri, M., Veillet, S., van Beuningen, L., Isaac, P., Edwards,  
 1029 K., Phillips, R.L., 2002 Toward positional cloning of Vgt1, a QTL controlling the transition from  
 1030 the vegetative to the reproductive phase in maize 13.
- 1031 Saxena, R.K., Edwards, D., Varshney, R.K., 2014. Structural variations in plant genomes. *Brief. Funct.*  
 1032 *Genomics* 13, 296–307. <https://doi.org/10.1093/bfpg/elu016>
- 1033 Schnable, P.S., Ware, D., Fulton, R.S., Stein, J.C., Wei, F., Pasternak, S., Liang, C., Zhang, J., Fulton, L.,  
 1034 Graves, T.A., et al., 2009. The B73 Maize Genome: Complexity, Diversity, and Dynamics. *Science*  
 1035 326, 1112–1115. <https://doi.org/10.1126/science.1178534>
- 1036 Shen, X., Liu, Z.-Q., Mocoer, A., Xia, Y., Jing, H.-C., 2015. PAV markers in Sorghum bicolor: genome  
 1037 pattern, affected genes and pathways, and genetic linkage map construction. *Theor. Appl.*  
 1038 *Genet.* 128, 623–637. <https://doi.org/10.1007/s00122-015-2458-4>
- 1039 Springer, N.M., Ying, K., Fu, Y., Ji, T., Yeh, C.-T., Jia, Y., Wu, W., Richmond, T., Kitzman, J., Rosenbaum, H.,  
 1040 et al., 2009. Maize Inbreds Exhibit High Levels of Copy Number Variation (CNV) and  
 1041 Presence/Absence Variation (PAV) in Genome Content. *PLoS Genet.* 5, e1000734.  
 1042 <https://doi.org/10.1371/journal.pgen.1000734>
- 1043 Stjernqvist, S., Rydén, T., Sköld, M., Staaf, J., 2007. Continuous-index hidden Markov modelling of array  
 1044 CGH copy number data. *Bioinformatics* 23, 1006–1014.  
 1045 <https://doi.org/10.1093/bioinformatics/btm059>

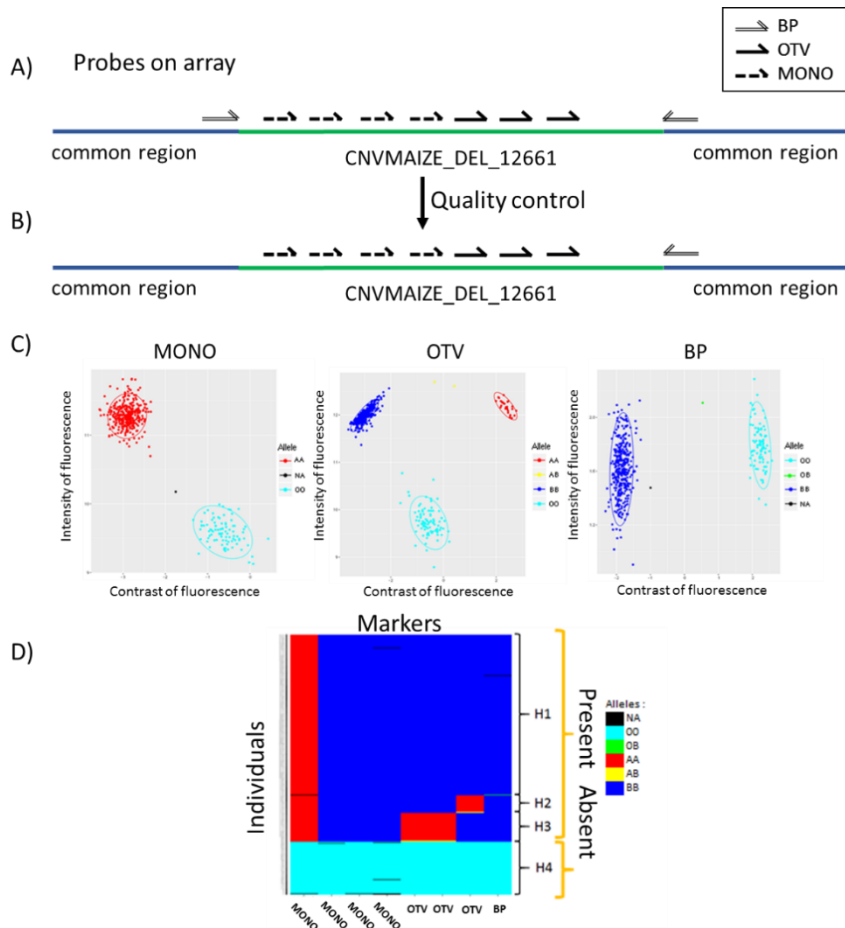
- 1046 Sun, S., Zhou, Y., Chen, J., Shi, J., Zhao, Haiming, Zhao, Hainan, Song, W., Zhang, M., et al., 2018.  
1047 Extensive intraspecific gene order and gene structural variations between Mo17 and other  
1048 maize genomes. *Nat. Genet.* 50, 1289–1295. <https://doi.org/10.1038/s41588-018-0182-0>  
1049 Swanson-Wagner, R.A., Eichten, S.R., Kumari, S., Tiffin, P., Stein, J.C., Ware, D., Springer, N.M., 2010.  
1050 Pervasive gene content variation and copy number variation in maize and its undomesticated  
1051 progenitor. *Genome Res.* 20, 1689–1699. <https://doi.org/10.1101/gr.109165.110>  
1052 Tai, T.H., Tanksley, S.D., 1990. A rapid and inexpensive method for isolation of total DNA from  
1053 dehydrated plant tissue. *Plant Mol. Biol. Report.* 8, 297–303.  
1054 <https://doi.org/10.1007/BF02668766>  
1055 Tuzun, E., Sharp, A.J., Bailey, J.A., Kaul, R., Morrison, V.A., Pertz, L.M., Haugen, E., Hayden, H., Albertson,  
1056 D., Pinkel, D., et al., 2005. Fine-scale structural variation of the human genome. *Nat. Genet.* 37,  
1057 727–732. <https://doi.org/10.1038/ng1562>  
1058 Unterseer, S., Bauer, E., Haberer, G., Seidel, M., Knaak, C., Ouzunova, M., Meitinger, T., Strom, T.M.,  
1059 Fries, R., Pausch, H., et al., 2014. A powerful tool for genome analysis in maize: development  
1060 and evaluation of the high density 600 k SNP genotyping array. *BMC Genomics* 15, 823.  
1061 <https://doi.org/10.1186/1471-2164-15-823>  
1062 Unterseer, S., Seidel, M.A., Bauer, E., Haberer, G., Hochholdinger, F., Opitz, N., Marcon, C., Baruch, K.,  
1063 Spannagl, M., Mayer, K.F., 2017. European Flint reference sequences complement the maize  
1064 pan-genome. *bioRxiv* 103747.  
1065 Varshney, R.K., Saxena, R.K., Upadhyaya, H.D., Khan, A.W., Yu, Y., Kim, C., Rathore, A., Kim, D., Kim, J.,  
1066 An, S., et al., 2017. Whole-genome resequencing of 292 pigeonpea accessions identifies genomic  
1067 regions associated with domestication and agronomic traits. *Nat. Genet.* 49, 1082–1088.  
1068 <https://doi.org/10.1038/ng.3872>  
1069 Waterhouse, R.M., Seppey, M., Simão, F.A., Manni, M., Ioannidis, P., Klioutchnikov, G., Kriventseva, E.V.,  
1070 Zdobnov, E.M., 2018. BUSCO Applications from Quality Assessments to Gene Prediction and  
1071 Phylogenomics. *Mol. Biol. Evol.* 35, 543–548. <https://doi.org/10.1093/molbev/msx319>  
1072 Ye, K., Schulz, M.H., Long, Q., Apweiler, R., Ning, Z., 2009. Pindel: a pattern growth approach to detect  
1073 break points of large deletions and medium sized insertions from paired-end short reads.  
1074 *Bioinformatics* 25, 2865–2871. <https://doi.org/10.1093/bioinformatics/btp394>  
1075 Zhao, Q., Feng, Q., Lu, H., Li, Y., Wang, A., Tian, Q., Zhan, Q., Lu, Y., Zhang, L., Huang, T., et al., 2018. Pan-  
1076 genome analysis highlights the extent of genomic variation in cultivated and wild rice. *Nat.*  
1077 *Genet.* <https://doi.org/10.1038/s41588-018-0041-z>  
1078 Zhou, P., Silverstein, K.A.T., Ramaraj, T., Guhlin, J., Denny, R., Liu, J., Farmer, A.D., Steele, K.P., Stupar,  
1079 R.M., Miller, J.R., et al., 2017. Exploring structural variation and gene family architecture with De  
1080 Novo assemblies of 15 Medicago genomes. *BMC Genomics* 18. [https://doi.org/10.1186/s12864-](https://doi.org/10.1186/s12864-017-3654-1)  
1081 [017-3654-1](https://doi.org/10.1186/s12864-017-3654-1)  
1082

1083 **List of Table and Figure**

1084 **List of figure**

1085





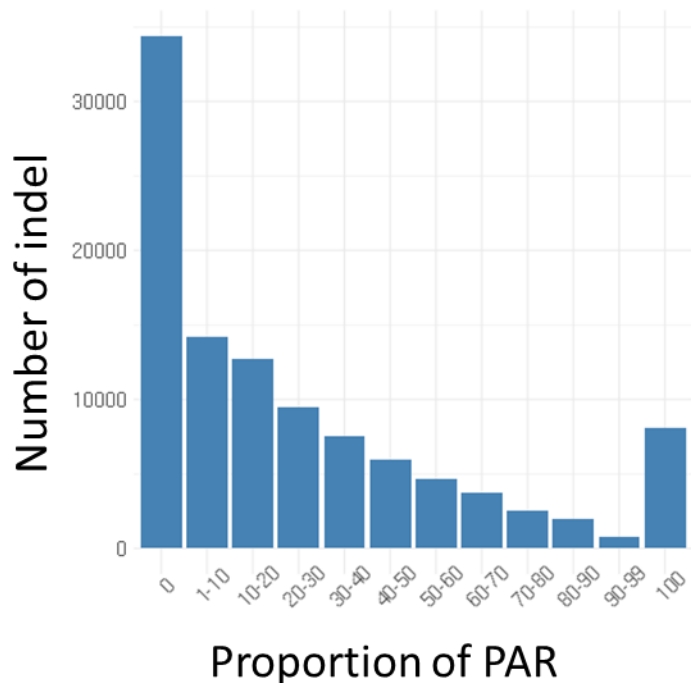
1086

1087 **Figure 1:** Genotyping of indel CNVMAIZE\_DEL\_12661 using three probe types on 445 individuals.  
 1088 A) Schematic distribution of the 9 probes along the sequence of indel CNVMAIZE\_DEL\_12661  
 1089 (green line) and the bordering sequence common between all individuals (blue line) genotyped by  
 1090 the array. Double, dotted, and full arrows represented the probes designing on the forward and  
 1091 reverse flanking sequences of the breakpoint sites (BP), at not polymorphic (MONO) and  
 1092 polymorphic sites (OTV) within internal sequence of indel. B) Schematic distribution of the 8  
 1093 probes passing Affymetrix® quality control and called by Affymetrix® pipeline C) Clustering  
 1094 produced by Affymetrix® algorithm for an OTV, MONO and BP probe from indel based on both  
 1095 fluorescence contrast (X axis) and intensity (Y axis) of the 445 inbred lines. Red, blue and yellow  
 1096 dots indicated the presence of the sequence (genotype “present”) either homozygous for allele A  
 1097 (AA), or allele B (BB) or heterozygous (AB), respectively. Cyan and green indicated that the  
 1098 sequence were absent in the individual (OO), or only in one copy of the sequence, e.g hemizygous  
 1099 for presence/absence (OB or OA). Black dots indicated individuals for which no genotype could be  
 1100 assigned (Missing data) D) Haplotypes displayed by the genotyping using 8 probes (column) on the  
 1101 445 inbred lines (row). Colors corresponded to the genotype of individuals produced by clustering  
 1102 in C)

1103

1104

1105



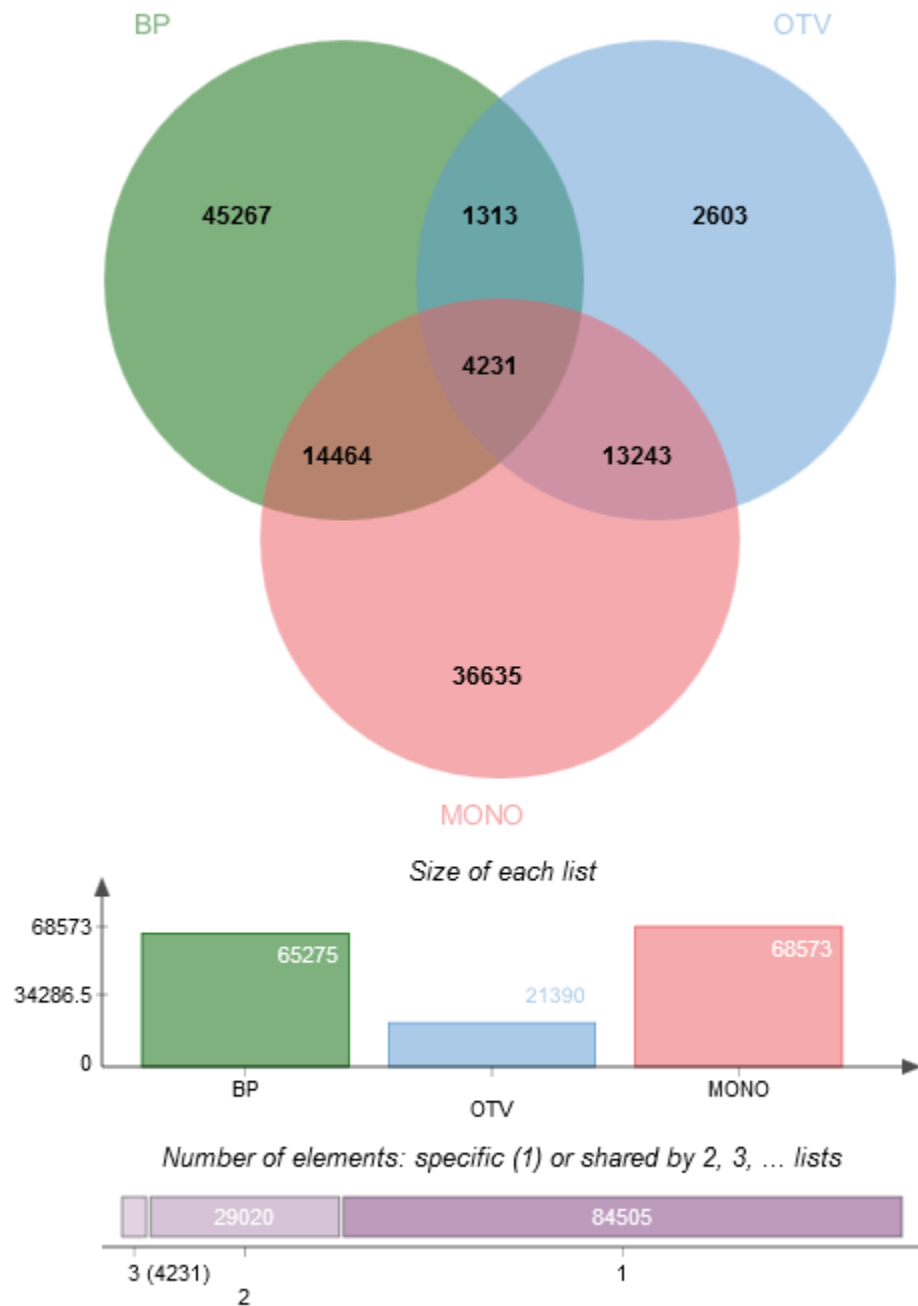
1106

1107 Figure 2: Distribution of the number of indels genotyped by the array according to the proportion  
1108 of presence/absence regions (Specific fraction) identified in their internal sequence.

1109

1110

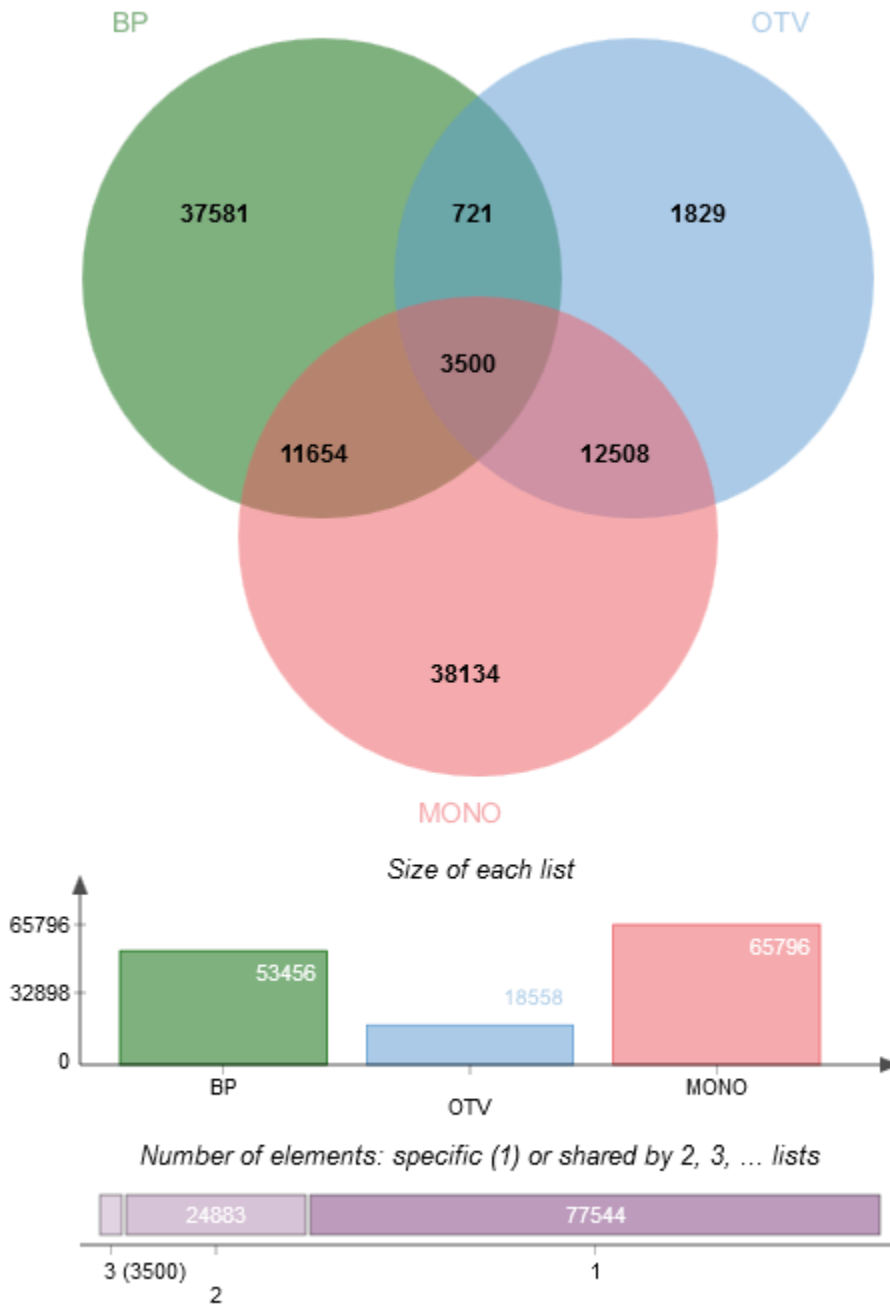
1111 A)



1112

1113

1114 B)

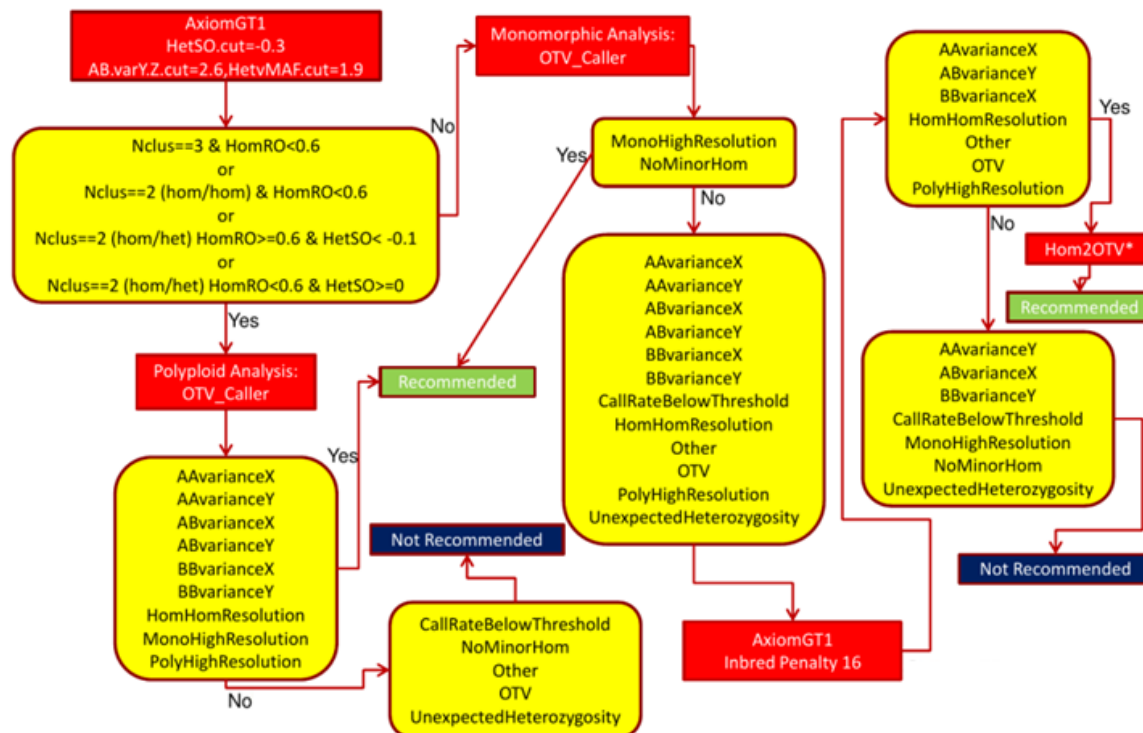


1115

1116 Figure 3: Number of indels that could be targeted by each type of probes designed (A) and selected  
1117 to be included in the final array (B).

1118

1119

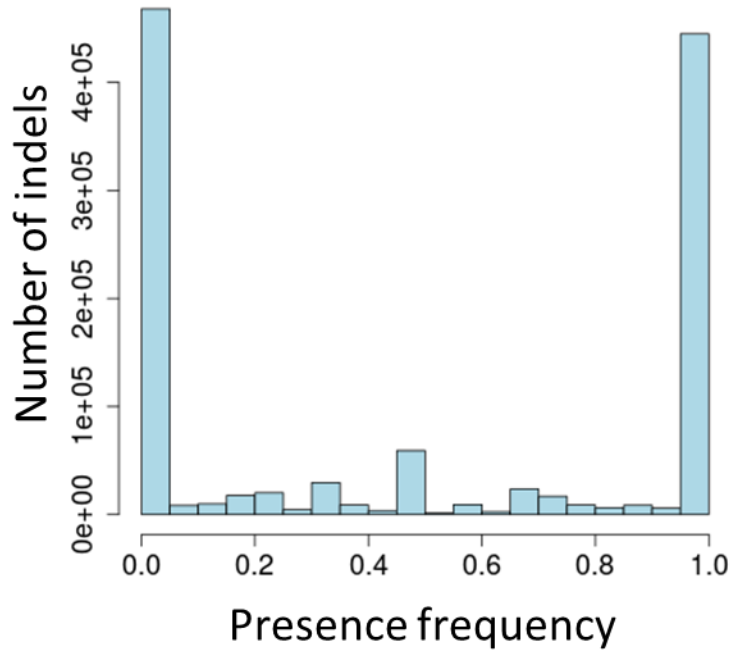


1120

1121 Figure 4: Dedicated Affymetrix® pipeline used for calling indel polymorphisms from the  
 1122 fluorescent intensity variation of MONO probes. Each probe was classified into different categories  
 1123 according to the number of cluster, the call rate and quality metrics of the clustering based on the  
 1124 position, variance and separation of different cluster. In order to retrieve the best clustering for  
 1125 each probes, successive step of clustering using different clustering algorithms (Red square, Axiom  
 1126 GT1, OTV caller, Hom2OTV) or/and with different parameters. According to their classification at  
 1127 each step (yellow square) and threshold used for quality metrics, probes could be classified as  
 1128 recommended (green square), not recommended (blue square) or to be submitted to another step.  
 1129 A new pipeline and an algorithm (Hom2OTV) have to be specifically developed for calling indel  
 1130 genotype of MONO probes since we expected only 2 clusters (absence / presence) that varied  
 1131 exclusively for fluorescent intensity rather than for fluorescent intensity ratio between two labelled  
 1132 nucleotides. At the end, all probes were classified into 14 categories either as recommended or not  
 1133 recommended depending on threshold.

1134

1135

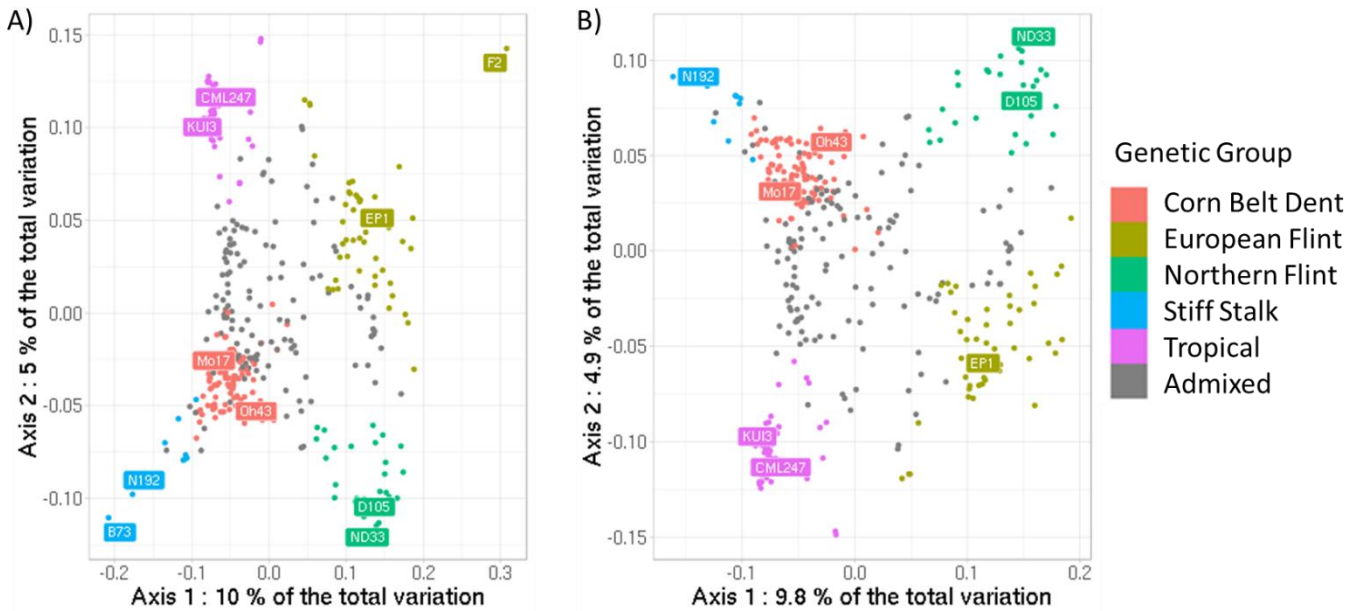


1136

1137 Figure 5: Distribution of the average allelic frequencies of the presence across different probes  
1138 within 48,486 indels with at least two probes genotyped for 24 inbred lines.

1139

1140



1141

1142 Figure 6: Principal coordinate analysis on the genetic distance (1-IBS) between inbred lines from an  
 1143 association panel estimated by 57,824 indels. A) 362 maize inbred lines were represented B) 360  
 1144 maize inbred lines were represented excluding B73 and F2 that are used for discovering indels.  
 1145 Colors represented the assignation of the inbred lines to the 5 genetic groups defined by admixture  
 1146 using Panzea SNPs from 50K Illumina array when the probability of assignation to a group  
 1147 (membership) were superior to 60%. Inbred lines that are not assigned to a group  
 1148 (membership<60%) were considered admixed. Common name of two maize accessions typical of  
 1149 each genetic groups were indicated.

1150

1151

## 1152 List of Table

1153 Table 1: F2, PH207 and C103 de novo assembly metrics. For each assembled genome are detailed: the number of scaffold sequences which  
 1154 were assembled, the length of the shortest scaffold, the length of the longest scaffold, the average size, the N50 of the assembly, the total  
 1155 number of bases included in the assembly, the percentage of Ns present in the assembly and finally the BUSCO statistics including the  
 1156 percentage of complete (C), fragmented (F) and missing (M) BUSCO genes from a total of 1440 BUSCO groups searched for maize.

Maize line	Number of scaffolds	Min size	Max size	Average size	N50	Total (Mb)	% of Ns	Complete BUSCOs (C)	Fragmented BUSCOs (F)	Missing BUSCOs (M)
<b>F2</b>	76563	892	112956	16900	14042	646.3	9.48%	89.3%	4.9%	5.8%
<b>PH207</b>	81688	884	2024489	29557	16860	797.5	8.90%	91.8%	2.7%	5.5%
<b>C103</b>	84990	886	120582	19305	16146	793	8.21%	90.6%	4.2%	5.2%

1157

1158 Table 2: Number of probes before and after selection for array design and passing the Affymetrix® quality control. At each step, are  
 1159 detailed the number (and percentage) of each probe type and the corresponding number (and percentage) of targeted indels. Note that a  
 1160 same indel could be genotyped by several probe types which conducted to a sum of percentage superior to 1 in indel columns.

	Before selection		On array		Called by Affymetrix® pipeline	
	Probes	indel	Probes	indel	Probes	indel
<b>BP_Type1</b>	6,648 (0.02%)	3,324 (2.82%)	4,691 (0.71%)	2,751 (2.6%)	2,092 (0.44%)	1,482 (1.66%)
<b>BP_Type2</b>	51,770 (0.2%)	25,885 (21.98%)	38,790 (5.85%)	22,662 (21.39%)	20,540 (4.29%)	14,407 (16.12%)
<b>BP_Type3</b>	71,820 (0.27%)	35,910 (30.5%)	41,272 (6.23%)	27,897 (26.34%)	23,631 (4.93%)	18,485 (20.68%)
<b>BP_Type4</b>	312 (0.001%)	156 (0.13%)	241 (0.04%)	146 (0.14%)	119 (0.02%)	93 (0.1%)
<b>OTV</b>	872,324 (3.26%)	21,390 (18.16%)	163,278 (24.64%)	18,558 (17.52%)	96,867 (20.22%)	15,064 (16.85%)
<b>MONO</b>	25,735,797 (96.25%)	68,573 (58.23%)	414,500 (62.54%)	65,796 (62.11%)	335,778 (70.1%)	63,597 (71.14%)
<b>ALL</b>	26,738,671	117,756	662,772	105,927	479,027	89,393

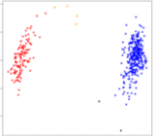
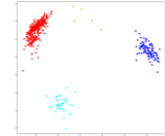
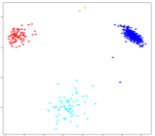
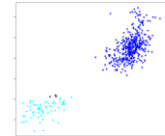
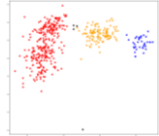
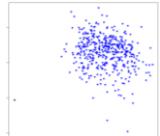
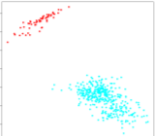
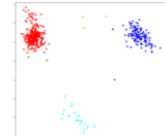
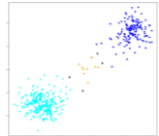
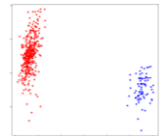
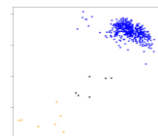
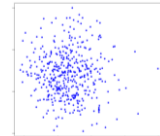
1161

Comment citer ce document :

MABIRE, C., Jorge, Darracq, A., Pirani, A., Rimbart, Madur, D., Combes, V., Vitte, C., Praud, Rivière, Joets, J., Pichon, Nicolas Dimitri, S. (2018). High throughput genotyping of structural variations in a complex plant genome using an original Affymetrix® Axiom® array. BioRxiv. , DOI : 10.1101/507756



1162 Table 3: Comparison between the clustering expected for BP, MONO and OTV probe type and the clustering produced by Affymetrix®  
 1163 pipelines based on the fluorescent intensity and contrast of 445 inbred lines for 479,027 probes. Clustering example: typical example of  
 1164 clustering based on the fluorescent intensity (y-axis) and contrast (x-axis). Colors indicate the assignment of the individuals to different  
 1165 clusters identified by pipeline. Description: Brief characteristic of each classification based on the clustering of individuals (homoz.=  
 1166 homozygote, het=heterozygous, OT= off-target)

Classification based on the clustering produced by Affymetrix® pipelines and genotyping assignment							
Probe types		BP	OTV				
BP	Nbr (%)	20,370 (43.9%)	26,012 (56.1%)				
	Clustering example						
	Description	Two homoz. clusters	Two homoz. and one OT clusters				
OTV		OTV	MONO	SNP	monomorphic		
	Nbr (%)	78,799 (81.3%)	502 (0.5%)	17,562 (18.1%)	4 (0.0%)		
	Clustering example						
Description	Two homoz. and one OT clusters.	One homoz. and one OT clusters.	Two homoz. clusters.	One cluster			
MONO		MONO	OTV	Unexpected MONO 1	SNP	Unexpected MONO 2	monomorphic
	Nbr (%)	212,434 (63,3%)	15,690 (4,7%)	68,562 (20,4%)	1,981 (0.6%)	9,525 (2.8%)	27,586 (8.29%)
	Clustering example						
Description	One homoz. and one OT clusters	Two homoz. and one OT clusters.	One homoz., one OT and one het. clusters.	Two homoz. clusters.	One homoz. and one het. clusters.	One cluster	

Comment citer ce document :

MABIRE, C., Jorge, Darracq, A., Pirani, A., Rimbart, Madur, D., Combes, V., Vitte, C., Praud, Rivière, Joets, J., Pichon, Nicolas Dimitri, S. (2018). High throughput genotyping of structural variations in a complex plant genome using an original Affymetrix® Axiom® array. BioRxiv. , DOI : 10.1101/507756

1168 Table 4: Consistency rate between expected and observed genotype for 4 individuals used to  
 1169 discover indel, according to the three type of probes and the two different genotype expected:  
 1170 presence (P) or absence (A) of the sequence.

Probe types	Expected genotyping	B73	F2	C103	PH207	All individuals
<b>BP</b>	<b>A</b>	0.96	0.93	0.94	0.94	0.94
	<b>P</b>	0.96	0.95	0.95	0.95	0.95
<b>OTV</b>	<b>A</b>	0.85	0.89	0.80	0.78	0.83
	<b>P</b>	0.93	0.97	0.96	0.96	0.96
<b>MONO</b>	<b>A</b>	0.77	0.81	0.82	0.81	0.80
	<b>P</b>	0.90	0.98	0.94	0.94	0.95
<b>All probe types</b>	<b>A</b>	0.80	0.85	0.83	0.82	0.82
	<b>P</b>	0.92	0.97	0.94	0.94	0.95
	<b>A &amp; P</b>	<b>0.85</b>	<b>0.94</b>	<b>0.89</b>	<b>0.89</b>	<b>0.89</b>

1171